ECMWF COPERNICUS REPORT

Copernicus Atmosphere Monitoring Service

Upgrade verification note for the CAMS near-real time global atmospheric composition service

Evaluation of the e-suite (experiment gp1p) for the period November 2016 - May 2017

Issued by: KNMI

Date: 3 July 2017

Ref: CAMS84_2015SC2_D84.3.1.3_201706_esuite_v1

IMPLEMENTED BY ECMWF

Upgrade verification note for the CAMS near-real time global atmospheric composition service

Evaluation of the e-suite (experiment gp1p) for the period November 2016 - May 2017

AUTHORS:
T. ANTONAKAKI (AA), S. BASART (BSC), A. BENEDICTOW (METNO), A.-M. BLECHSCHMIDT (IUP-UB), S. CHABRILLAT (BIRA-IASB), Y. CHRISTOPHE (BIRA-IASB), H. CLARK (CNRS-LA), E. CUEVAS (AEMET), H. ESKES (KNMI), K. M. HANSEN (AU), U. IM (AU), J. KAPSOMENAKIS (AA), B. LANGEROCK (BIRA-IASB), K. PETERSEN (MPG), A. RICHTER (IUP-UB), M. SCHULZ (METNO), N. SUDARCHIKOVA (MPG), V. THOURET (CNRS-LA), A. WAGNER (MPG), C. ZEREFOS (AA)

REPORT OF THE COPERNICUS ATMOSPHERE MONITORING SERVICE, VALIDATION SUBPROJECT.

CITATION:
ESKES, H. J., T. ANTONAKAKI, S. BASART, A. BENEDICTOW, A.-M. BLECHSCHMIDT, S. CHABRILLAT, Y. CHRISTOPHE, H. CLARK, E. CUEVAS, K. M. HANSEN, U. IM, J. KAPSOMENAKIS, B. LANGEROCK, K. PETERSEN, A. RICHTER, M. SCHULZ, N. SUDARCHIKOVA, V. THOURET, A. WAGNER, C. ZEREFOS, UPGRADE VERIFICATION NOTE FOR THE CAMS NEAR-REAL TIME GLOBAL ATMOSPHERIC COMPOSITION SERVICE, COPERNICUS ATMOSPHERE MONITORING SERVICE (CAMS) REPORT, CAMS84_2015SC2_D84.3.1.3_201706_esuite_v1.pdf, JULY 2017.

STATUS:
VERSION 1, FINAL

DATE:
03/07/2017

Executive Summary

The Copernicus Atmosphere Monitoring Service (CAMS, http://atmosphere.copernicus.eu) is a component of the European Earth Observation programme Copernicus. The CAMS global near-real time (NRT) service provides daily analyses and forecasts of reactive trace gases, greenhouse gases and aerosol concentrations.

CAMS has a sub-project dedicated to the validation of the service products. The validation results for the CAMS global NRT service (the o-suite) products and high-resolution greenhouse gas simulations can be found in Eskes et al. (2017) and Eskes et al. (2015). The observational datasets used for this validation are described in Eskes et al. (2016). These validation reports and the verification websites can be found here: http://atmosphere.copernicus.eu/user-support/validation/verification-global-services.

This document contains an evaluation of the upgrade of the NRT service planned for the Summer 2017. Before the upgrade, the new model configuration (the e-suite) is operated in parallel to the operational NRT service (the o-suite) for about half a year. Below the main results are summarised from a comparison of the performance of the forecasts with the new e-suite run (experiment id "gp1p", period November 2016 - May 2017), the operational run (o-suite) and independent observations.

Noteable changes between this e-suite and the operational o-suite are the assimilation of PMAp AOD observations from METOP A&B over land and ocean, and updates in the modelling of aerosols. Section 1 provides a brief overview of the model changes between the e-suite and o-suite. Section 2 contains the figures that provide the evidence for the conclusions presented below.

Main conclusions

The new model configuration is an improvement as far as aerosols is concerned. Tropospheric ozone e-suite and o-suite results generally are very comparable, apart from a wintertime negative high-latitude bias (about 2-5 ppb) compared to the current operational version. This bias is largely related to changes (positive jump) in o-suite ozone that occurred on 24 January, the day of the last upgrade. In spring, ozone values in o-suite and e-suite are very similar. The other trace gas concentrations (CO, NO2, HCHO) show minor differences. Methane is improved.

Based on these results we can give an overall positive advice on the upgrade. At the same time it is of importance to better understand the origin of the tropospheric ozone differences between the e-suite and the two o-suite versions which are likely related to changes in the assimilation of ozone satellite data.

Global Aerosol

Taking the o-suite from March to May 2017 as reference, the following changes wrt to aerosol optical depth (AOD) can be found in the e-suite: AOD reductions (-7%) are seen both in Northern hemisphere pollution regions and dust regions. The largest changes that affect these areas are due

to sulphate and organic AOD, which are more concentrated to highly polluted areas (Fig. 2.1.1, 2.1.2). The sum of sulphate and organic AOD is reduced by about 50% in the e-suite, contributing to the overall reduction in AOD in e-suite. Also 50% less Black Carbon AOD is found, on the contrary Sea salt AOD is increased by 75 % in e-suite (Table 2.1.1).

The RMS error against daily Aeronet in MAM 2017 is slightly higher for the e-suite with a slightly worse spatial representation of the AOD field (Fig. 2.1.3). Statistics show a temporal-spatial RMS error increase from 0.133 (o-suite) to 0.141 (e-suite), but with a small reduction of MNMB going from 23% to 20%, respectively. The quality of the IFS e-suite, despite or because of the significant shift in the aerosol composition is better or as good as in the o-suite. Some features of the IFS model have changed: The Angström exponent did show an improvement and a change in size assumptions (Fig. 2.1.4). There is still a 20% AOD loss in the first 3 days of forecast indicating an initial day imbalance between emissions and removal introduced by the assimilation

Dust

From 1 December 2016 to 1 June 2017, e-suite shows comparable AOD (see Figure 2.1.5) and DOD (see Figure 2.1.6) results than o-suite despite e-suite increases the dust burden particularly in spring over the main desert dust sources in North Africa and the Middle East.

The e-suite is the model that best reproduces the DOD AERONET observations (correlation values of 0.79 for o-suite and 0.82 for e-suite and MB of -0.07 for o-suite and -0.06 for e-suite in average for all the AERONET sites) particularly in the Middle East and Sahel (see Table 2.1.1). The e-suite results are closer to the SDS-WAS Median Multimodel. CAMS o-suite and e-suite DOD underestimations are linked to a high ratio AOD/DOD over the Sahara and the Middle East is observed in both e-suite and o-suite (see Figure 2.1.5 and Figure 2.1.6).

Aerosol validation over the Mediterranean

From 1 December 2016 to 1 June 2017, e-suite shows results comparable to the o-suite although e-suite is the model that best reproduces the AOD daily variability of AERONET observations over the Mediterranean. In Western, Central and Eastern Mediterranean, the correlation coefficient increases from 0.63 to 0.66, from 0.75 to 0.76 and from 0.61 to 0.63, respectively for o-suite and e-suite. Overestimations in Western and Central Mediterranean shown in o-suite are corrected in e-suite with a decrease of MB from 0.02 for o-suite to 0.01 for e-suite (see MB in Figure 2.1.7).

Tropospheric ozone (O_3)

Model profiles of the CAMS runs were compared to free tropospheric balloon sonde measurement data of 38 stations taken from the NDACC, WOUDC, NILU and SHADOZ databases for December 2016 to February 2017 (see Fig. 2.2.1, 2.2.2, 2.2.3). The monthly averaged biases delivered by the e-suite upgrade show larger negative MNMBs over the Arctic and Northern Midlatitudes (o-suite between 4 and -11%, e-suite -8 and -23%). Over the Tropics and Antarctica there are no significant differences between the e-suite and the o-suite.

For the Near Real Time (NRT) validation, 12 GAW stations and 13 ESRL stations are currently delivering O_3 surface concentrations in NRT, and the data are compared to model results between

December 2016 and May 2017 (Fig. 2.2.4 to 2.2.6) for GAW, and October 2016 and March 2017 for ESRL (Fig. 2.2.7 and 2.2.8). For these stations, O_3 mixing ratios provided by the e-suite are lower than for the o-suite over the Arctic and Northern mid-latitudes stations. Especially for European stations the e-suite shows larger negative MNMBs (o-suite: between -1 and -7%, e-suite: between -7 and -19. Correlation coefficients are almost identical. In both Arctic and NH mid-latitudes sites after the middle of March the o-suite and the e-suite ozone concentrations are becoming similar. Over Tropical stations o-suite and the e-suite ozone concentrations are almost the same during all the validation period. Lastly it should be noted that over Lauder station in the New Zealand and Antarctica stations (ARH and SPO) O_3 mixing ratios provided by the e-suite are lower than for the o-suite from end of April onwards (SH cold season; see also Fig 2.2.8 lower right panel). Unfortunately at the moment of writing there are not available ESRL observations after 1 April to compare with the modelled O_3 values. Correlation coefficients are almost identical over all ESRL stations.

We note that during the previous upgrade, the e-suite showed larger tropospheric ozone values than the o-suite running at the end of 2016. This e-suite is the current o-suite, since 24 January 2017. The present e-suite is partly correcting for this increase by showing lower ozone. The jump in the o-suite values could be related to the data assimilation (See Fig. 2.2.13 which shows that the o-suite related control run has no jump).

Compared to IAGOS aircraft profiles, the e-suite has lower mixing ratios in the boundary layer and surface layer compared with the o-suite (Fig. 2.2.9, 2.2.10). In midlatitudes where ozone is already underestimated by the o-suite, the e-suite results in an increased negative bias (see fig 2.2.9: Paris and Frankfurt), but in tropical regions where ozone is overestimated by the o-suite, the reduction in mixing ratios in the e-suite results in an improvement (e.g. fig 2.2.10: Taipei).

Tropospheric ozone (O_3) in the Arctic

Surface ozone measurements from three Arctic sites were applied to evaluate the gp1p e-suite against the o-suite. The e-suite of the surface ozone for Alert, Svalbard and VRS in the Arctic has a larger negative bias (NMB = -0.19 to -0.26) than the o-suite (-0.09 to -0.18) for December 2016 - February 2017. Although the e-suite predicts lower concentrations than the o-suite for all sites the main part of the bias difference can be explained by the jump in the o-suite on January 24th that brings the o-suite closer to the measurements (Fig. 2.2.13). Overall, the e-suite shows a more consistent time evolution of ozone in this period than the o-suite. From the last part of February and onwards the o-suite and the e-suite are around the same level, see Fig. 2.2.12.

Tropospheric ozone (O_3) in the Mediterranean

In general e-suite simulated O_3 surface ozone concentration are about 1.5-2.5 ppb lower than o-suite O_3 surface ozone concentration in the Mediterranean area. Thus e-suite biases are slightly less positive/slightly more negative than o-suite, but there is no clear winner. In most of Mediterranean sites the differences between o-suite and e-suite can be explained by the jump in the o-suite on January 24th. It should be noted that after the middle of March the o-suite and the e-suite ozone concentrations are around the same level. E-suite and o-suite correlation coefficients are almost equal (Figure 2.2.11).

Tropospheric Carbon Monoxide (CO)

For the Near Real Time (NRT) validation, 11 GAW stations are currently delivering CO surface concentrations in NRT, and the data are compared to model results between December 2016 and February 2017 (Fig. 2.3.1 to 2.3.3). CO mixing ratios provided by the e-suite lead to similar MNMBs. The e-suite shows slightly larger negative MNMBs for stations in Europe, for Minamitorishima and for Cape Verde station. Correlation coefficients are a bit improved for stations in the Southern Hemisphere, but the differences are small.

The time-series of ozone at Frankfurt and Taipei compared to IAGOS aircraft observations (fig.2.3.4) shows that the e-suite and o-suite are almost identical. Monthly-mean profiles in figure 2.3.5 again show that there is virtually no difference between the two runs.

FTIR observations (NDACC, TCCON) show a bit more pronounced differences, sometimes with better, sometimes worse results depending on the site (Fig. 2.3.6, 2.3.7).

CO total columns from o-suite and e-suite CAMS simulations are compared with MOPITTv6 and IASI for different regions from November 2016 until March 2017 (Fig. 2.3.8 and 2.3.9). There is nearly no differences observed between o-suite and e-suite in CO total columns. The model simulations reproduce well the CO total columns observed from MOPITTv6 (within 5 %, apart for South Africa, South: within 10%, East Asia within 12%), while IASI total columns show lover CO total columns in the northern regions (Alaska Fire regions and Siberian Fire region) and higher CO total columns in North and South African Region compared to MOPITTv6 and the model simulations. In the South African Region, the CAMS simulations are closer to the IASI observations than to MOPITTv6 during the months of 2017. Comparison for the forecasts of day 2 and day 4 are shown in Figure 2.3.10, but show very little differences.

Tropospheric Nitrogen dioxide (NO_2)

The e-suite and o-suite perform very similar for comparisons against tropospheric NO_2 from GOME-2, there are only minor differences between both model runs. Time series in Figure 2.4.1 show that e-suite and o-suite underestimate tropospheric NO_2 over South Africa and underestimate the seasonal cycle over Europe compared to GOME-2. It is not clear if the ups and downs of wintertime GOME-2 values over Europe are realistic, although a quick inspection of daily GOME-2 satellite images did not point to problems regarding the retrieval. Gobal maps of tropospheric NO_2 for January 2017 (Figure 2.4.2) show that e-suite and o-suite strongly underestimate wintertime values over European anthropogenic emission areas and that shipping routes are more pronounced compared to GOME-2. Most of these issues are known in general from previous NRT reports.

UV-Vis MAX-DOAS observations at Xianghe (Fig. 2.4.3) confirm the small difference between o-suite and e-suite. During high peak events the differences are larger.

Formaldehyde (HCHO)

There is almost no difference between e-suite and o-suite, no major issues are found.

Model results and observations are in reasonable agreement for HCHO columns with respect to magnitude for time series shown in Figure 2.5.1. The underestimation of values over Eastern US

may result from a lack of satellite data (caused by instrument degradation) for this region during Northern Hemisphere winter months (see Figure 2.5.2 for an example). Global maps of tropospheric HCHO for January 2017 (Figure 2.5.2) show a rather good agreement between models and GOME-2, but both runs overestimate values over some parts of Australia and over forest fire regions in Central Africa.

Methane

TCCON methane observations show that the e-suite reduces the bias, as compared to the o-suite, at all sites from 3-4% to values of about 2-3% and is a clear improvement (Fig 2.8.1).

Stratospheric ozone

The e-suite "gp1p" is globally very similar to o-suite for the considered period from October 2016 to April 2017, see Fig. 2.6.3. The validation with ozone sondes (Fig. 2.6.1, 2.6.2, 2.2.3) and with NDACC microwave observations (Fig. 2.6.5) confirms this.

Also when compared to satellite observations (Fig 2.6.4) in the pressure range of 1hPa to 100hPa, e-suite and o-suite are very comparable with the notable exception in the period between 19 Dec 2016 and 9 Jan 2017, where the divergences were mostly marked in the southern hemisphere (Fig. 2.6.3).

For the 4th day forecast (96 to 120hours), there is an improvement in the middle-upper stratosphere (approx 1-6 hPa) where the e-suite is closer to the observations, mainly in the southern hemisphere up to Jan 2017 (Fig 2.6.4).

Stratospheric Nitrogen dioxide (NO_2)

Stratospheric chemistry is not implemented in CIFS and hence models are not expected to show reasonable results for stratospheric NO_2. However, it is surprising that the o-suite is closer to the satellite observations since the update in Jan 2017 than the e-suite, which strongly understimates stratospheric NO_2 as previous model versions (Fig. 2.7.1). At least in previous model versions of the o-suite, the only constraint on stratospheric NOx was implicitly made by fixing the HNO_3 to O_3 ratio at the 10 hPa level.

Table of Contents

1. Description of the o-suite and e-suite

Below a short model description is given on both the CAMS o-suite operational data-assimilation and forecast run and the new e-suite.

1.1 o-suite

The o-suite consists of the C-IFS-CB05 chemistry combined with the CAMS bulk aerosol model. The chemistry is described in Flemming et al. (2015), aerosol is described by the bulk aerosol scheme (Morcrette et al., 2009). Dissemination of the CAMS o-suite forecasts is two 5-day forecasts per day, based on 00UTC and 12UTC analyses. The o-suite data is also stored under expver ”0001” of class ”MC” of the MARS archiving system of ECMWF. The latest update of the o-suite occured on 24 January 2017. Information on the model versions can be found at http://atmosphere.copernicus.eu/user-support/operational-info .

Here a summary of the main specifications of this version of the o-suite is given:

- The meteorological model is based on IFS version CY43R1; the model resolution is T511 (approx. 40 km) with 60 vertical layers.
- The CB05 tropospheric chemistry is used (Williams et al., 2013), originally taken from the TM5 chemistry transport model (Huijnen et al., 2010)
- Stratospheric ozone during the forecast is computed from the Cariolle scheme (Cariolle and Teyssèdre, 2007) as already available in IFS, while stratospheric NOx is constrained through a climatological ratio of HNO3/O3 at 10 hPa.
- Monthly mean dry deposition velocities are based on the SUMO model provided by the MOCAGE team, with a resolution of 1.0×1.0 degree.
- The aerosol model includes 12 prognostic variables, which are 3 bins for sea salt and desert dust, hydrophobic and hydrophilic organic matter and black carbon, sulphate aerosols and its precursor trace gas SO_2 (Morcrette et al., 2009).
- Data assimilation is described in Inness et al. (2015) and Benedetti et al. (2009) for chemical trace gases and aerosol, respectively. A variational bias correction is used (Dee and Uppala, 2009). The data sets assimilated can be found in Table 1.1.
- Year-specific anthropogenic emissions are based on the MACCity emissions (Granier et al., 2011). Biogenic emissions originate from POET. Only for isoprene, a climatology of the MEGAN-MACC emission inventory (Sindelarova et al., 2014) is adopted. Resolution of emissions is 0.5×0.5 degree.
- NRT fire emissions are taken from GFASv1.2 (Kaiser et al. 2012), both for gas-phase and aerosol, available on 0.1×0.1 degree.
- Since 21 June 2016, two 5-day forecasts are produced per day (instead of one), based on 00UTC and 12UTC analyses. The 12UTC forecast will be available before 22UTC.

- Since 21 June 2016 there is a shift in the data assimilation windows from 9UTC-21UTC to 3UTC-15UTC, and from 21UTC-9UTC to 15UTC-3UTC.

Before 3 September 2015 the o-suite used an older meteorological cycle (CY40r2) and run under experiment (EXPVER) ”g4e2”. Before 18 September 2014 the o-suite was based on the coupled IFS-MOZART system (Stein et al., 2013), running under expid ”fnyp”.

Table 1.1: Satellite retrievals of reactive gases and aerosol optical depth that are actively assimilated in the o-suite.

Instrument	Satellite	Provider	Version	Type	Status
MLS	AURA	NASA	V3.4	O3 Profiles	20130107 -
OMI	AURA	NASA	V883	O3 Total column	20090901 -
GOME-2A	Metop-A	Eumetsat	GDP 4.7	O3 Total column	20131007 -
GOME-2B	Metop-B	Eumetsat	GDP 4.7	O3 Total column	20140512 -
SBUV-2	NOAA	NOAA	V8	O3 21 layer profiles	20121007 -
IASI	MetOp-A	LATMOS/ULB	-	CO Total column	20090901 -
IASI	MetOp-B	LATMOS/ULB	-	CO Total column	20140918 -
MOPITT	TERRA	NCAR	V5-TIR	CO Total column	20130129-
OMI	AURA	KNMI	DOMINO V2.0	NO2 Tropospheric column	20120705 -
OMI	AURA	NASA	v003	SO2 Tropospheric column	20120705-20150901
GOME-2A/2B	METOP A/B	Eumetsat	GDP 4.7	SO2 Tropospheric column	20150902-
MODIS	AQUA / TERRA	NASA	Col. 5 Deep Blue	Aerosol total optical depth	20090901 - 20150902 -
OMPS	Suomi-NPP	NOAA / EUMETSAT		O3 profile	
PMAp	METOP A	EUMETSAT		AOD	

1.2 e-suite

The e-suite with experiment ID "**gp1p**" has been running for the period starting from October 2016 to the present day. The description of the system is given at http://atmosphere.copernicus.eu/implementation-ifs-cycle-43r3cams#document_versions.

The e-suite is based on ECMWF's IFS cycle 43R3 (for the o-suite this is cycle 43R1), https://software.ecmwf.int/wiki/display/FCST/Implementation+of+IFS+cycle+43r3.

The main CAMS composition-related changes are:

Data assimilation:

- **Assimilation of PMAp aerosol optical depth (AOD) from METOP-A and METOP-B over land and ocean.** The Polar Multi-Sensor Aerosol Product (PMAp) is a combined aerosol product based on measurements by the GOME-2, AVHRR and IASI instruments. PMAp data over land and PMAp data from METOP-B are introduced in this cycle. The impact of PMAp on the analysis and subsequent forecast is low, but at the same time important to increase resilience against potential failures of the two MODIS instruments.

Modelling:

- **Updated optical properties for aerosol.** This has a small impact on the optical depth of organic matter and of sea-salt: both are less extinctive per unit mass.
- **Bug fix for sedimentation speed for sea-salt.** Impact on sea salt burden and AOD.
- **Improved parameterisations for SO2 and SO4 dry deposition and SO2 to SO4 conversion.** These changes have an impact on the suphate aerosol burden and AOD.
- **Improved use of ozone information in UV processor.** The use of ozone information from the IFS model has been improved in the UV processor resulting in changes to both the spectrally resolved UV radiation and the UV-Index for all-sky and clear-sky conditions.
- **Update of solar radiation input for UV processor.** The spectrally resolved solar radiation climatology has been updated to ATLAS3. This results in gerenally lower UV values that better match surface observations.

2. Upgrade evaluation results: e-suite versus o-suite

2.1 Aerosol evaluation

2.1.1 Total AOD

The evaluation is done for December 2016 to May 2017, which were available fully at the time of evaluation. AeroCom tools have been applied and image catalogues are available at http://aerocom.met.no/cgi-bin/aerocom/surfobs_annualrs.pl?PROJECT=CAMS&MODELLIST=CAMS-e-suite.

Only the MAM 2017 figures are shown as sulphate AOD reduced and organic AOD changed already quite a bit when the o-suite changed in January 2017, reducing sulphate AOD by 30%, but increasing organic AOD 100%. The e-suite (experiment ECMWF_GP1P) seems to simulate less global aerosol optical thickness (AOD) than the recent and current o-suite (March-May 2017 o-suite: 0.160 vs e-suite: 0.148). However the maps in figures 2.1.1 and 2.1.2 indicate that there is in particular less sulphate and somewhat less organic AOD overall, more concentrated in polluted areas. Sea salt AOD is increased by 75% in e-suite and black carbon AOD is overall decreased, but more concentrated. The Angström Exponent as shown in Figure 2.1.4 supports the idea that the size of the aerosol is better taken into account in the e-suite.

Table 2.1.1 Mean global total and speciated AOD in e-suite and o-suite for winter (December, January and February) 2016/17 and spring (March, April and May) 2017. Less total AOD in e-suite mainly due to overall less sulphate. Noteworthy is the largest changes to sulphate and organic AOD in winter 2016/17 due to January 2017 update of o-suite.

	DJF2016/2017		**MAM2017**	
	e-suite	**o-suite**	**e-suite**	**o-suite**
OD550_AER	0.128	0.138	0.148	0.160
OD550_BC	0.005	0.009	0.005	0.011
OD550_DUST	0.012	0.015	0.025	0.023
OD550_OA	0.042	0.035	0.048	0.054
OD550_SO4	0.028	0.057	0.029	0.048
OD550_SS	0.042	0.023	0.042	0.024

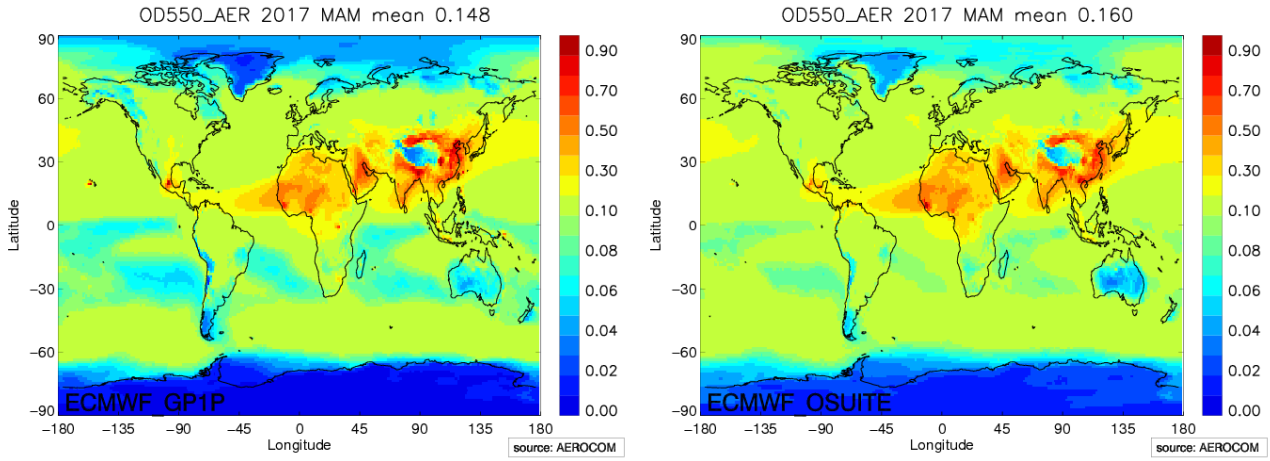

Fig. 2.1.1. Averaged aerosol optical depth (AOD) from e-suite (left) and o-suite (right) IFS model for March-May2017. Mean AOD in e-suite is at 0.148, which is 7% less than what was in the o-suite. E-suite reductions are seen in particular in remote regions.

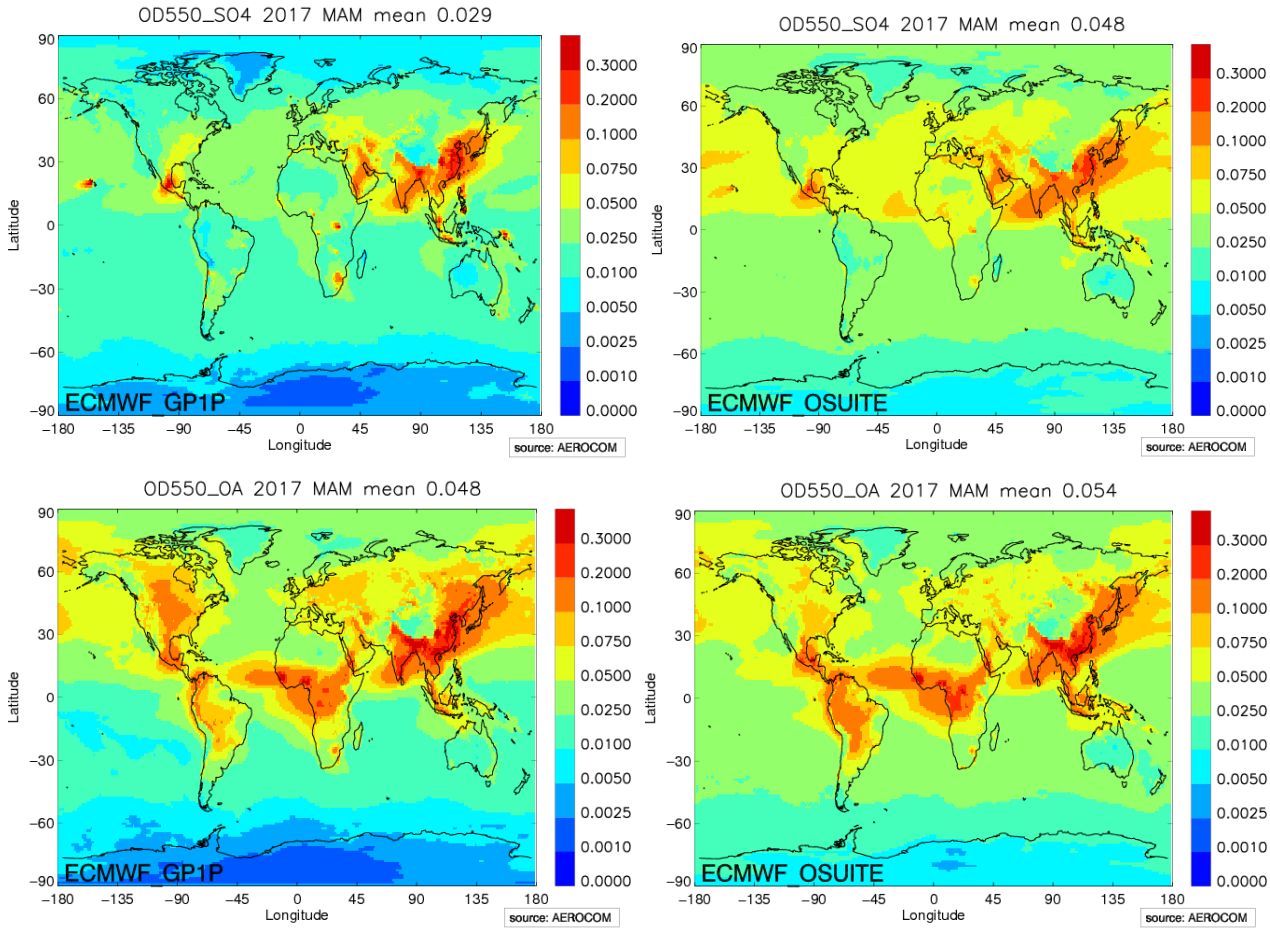

Fig. 2.1.2. Averaged sulfate optical depth in upper row (e-suite (left) and o-suite (right)) and organic aerosol optical depth lower row, for March-May 2017. In the e-suite sulphate AOD is more concentrated in polluted areas compared to the o-suite, with significant reductions in remote areas. Organic AOD are almost equal in the two suites, but for the e-suite values have increased more in remote areas and in the Southern hemisphere.

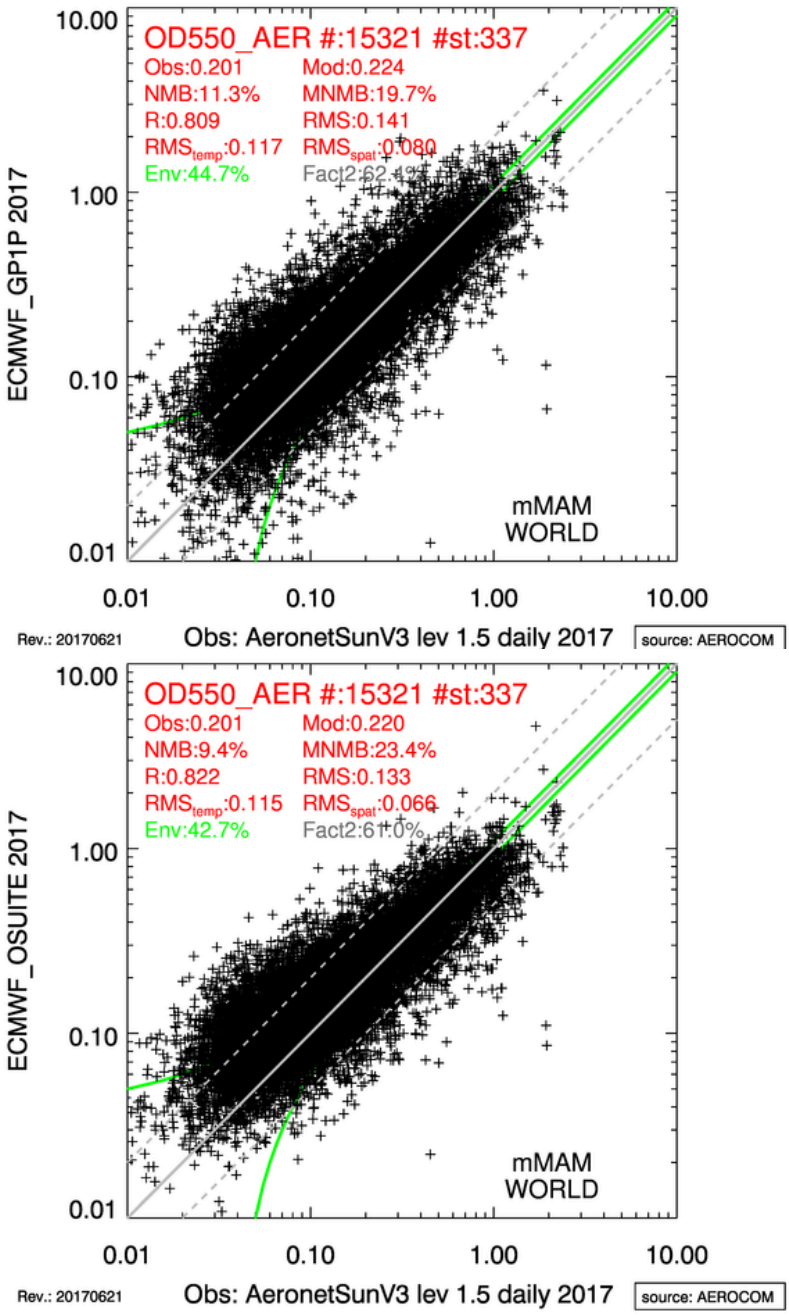

Fig. 2.1.3. Evaluation of simulated daily AOD against Aeronet NRT version 3, level 1.5 photometer measurements in e-suite (top) and o-suite (bottom) for the period March-May 2017. Statistics shown in the figure show a temporal-spatial RMS error increase from 0.133 to 0.141 and a reduction of MNMB from 23% to 20%. The decomposition of the RMS error into a spatial and temporal component indicates that the increase in RMS in the e-suite is mainly due to a less good spatial distribution of AOD. A small positive bias in o-suite is still present in the e-suite. The quality of the IFS e-suite, despite or because of the shift in the aerosol composition is almost as good as the o-suite.

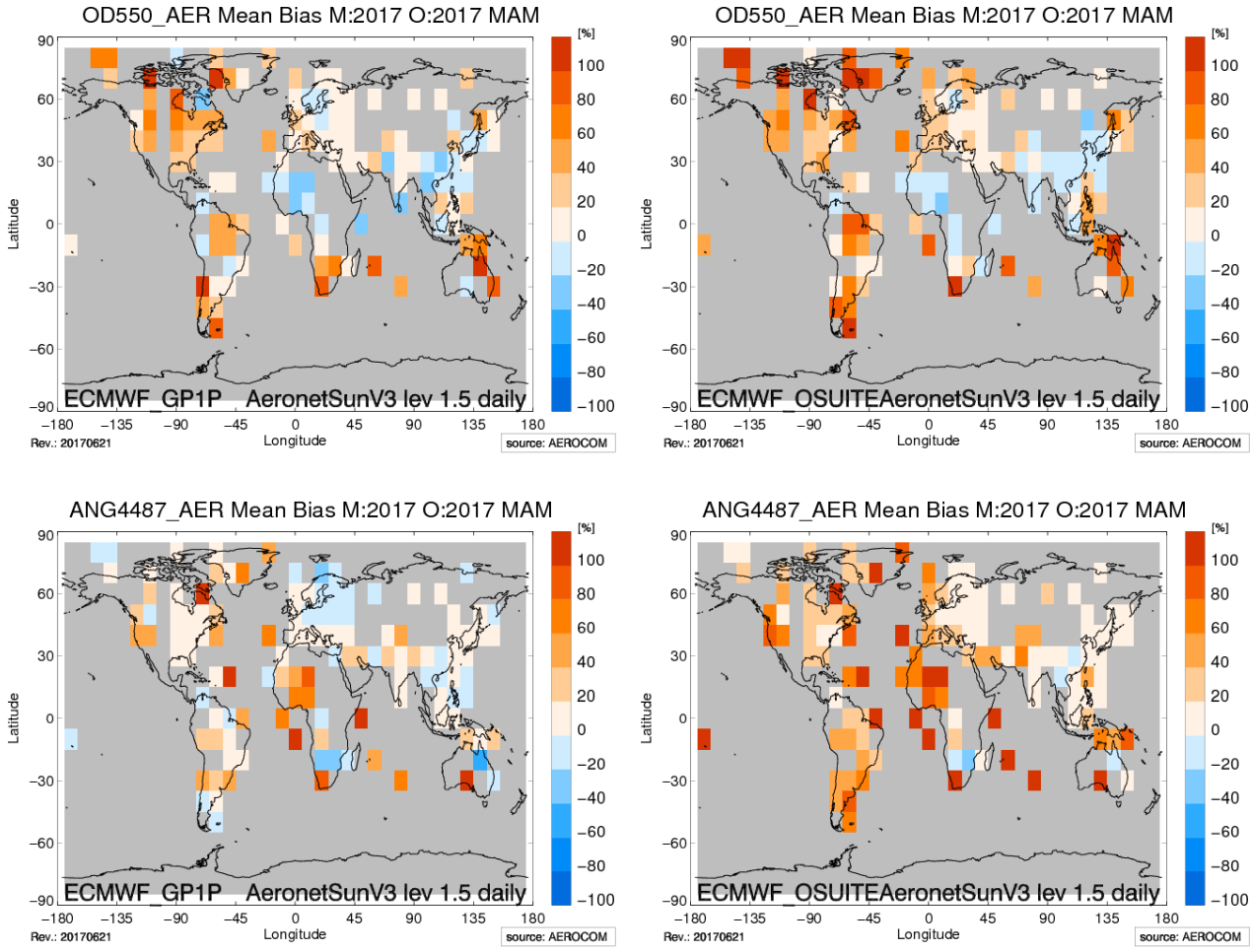

Fig. 2.1.4. Regional relative mean bias of simulated daily AOD against NRT level 1.5 Aeronet SunV3 photometer measurements in e-suite (left) and o-suite (right) for the period March-May 2017. Most regions exhibit an AOD bias between +-40%, supporting that the e-suite, despite or because of the shift in the aerosol composition is as good as the o-suite. Corresponding figures for the Angström Exponent are shown below. The bias is significantly reduced.

2.1.2 Dust

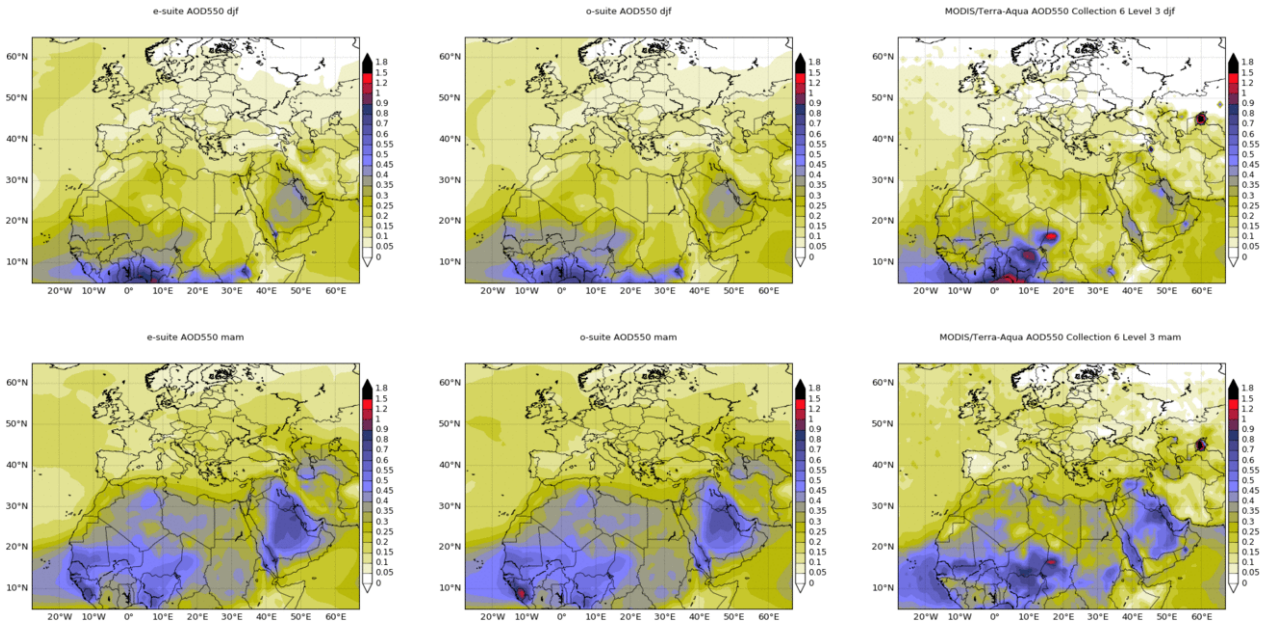

Figure 2.1.5: Averaged AOD 24h forecast from e-suite (right) and o-suite (central) as well as AOD combined Dark Target and Deep Blue MODIS Aqua/Terra Level 3 Collection 6 (left) for winter (DJF, top row) and spring (MAM, bottom row). Major aerosol activity is concentrated over the Sahara (in the Bodelé Basin and the Mali/Mauritania border as well as Magrebh) and the Arabian Peninsula. Overall, CAMS e-suite shows comparable results than o-suite in good agreement with MODIS AOD.

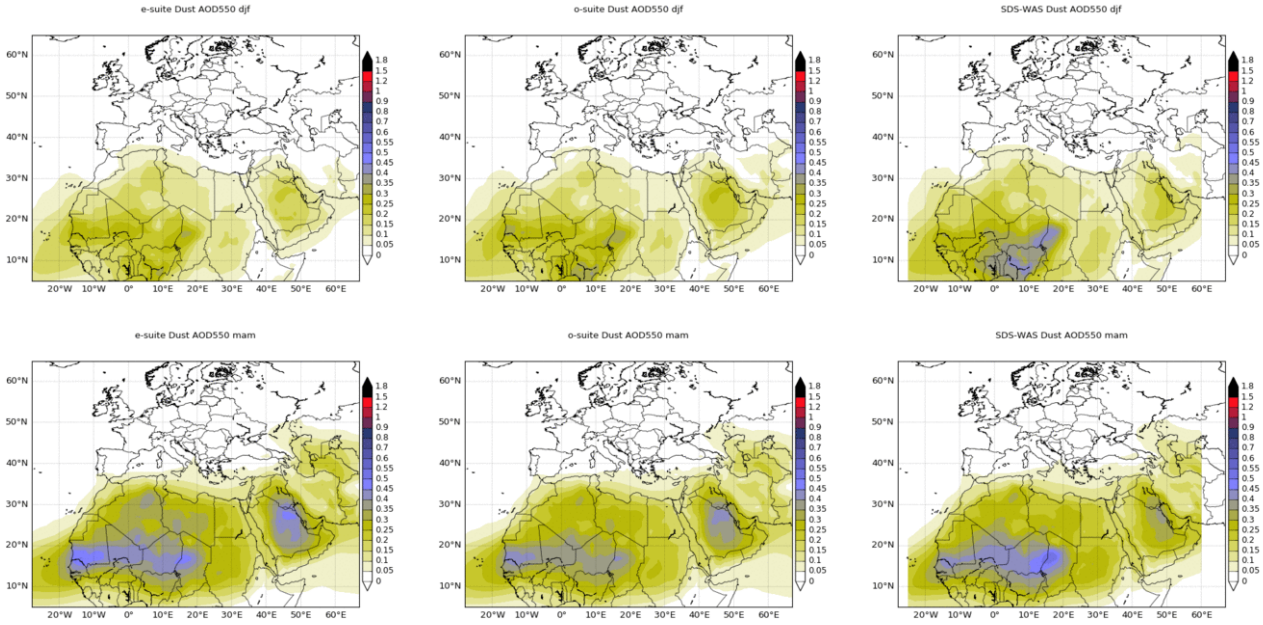

Figure 2.1.6: Averaged DOD 24h forecast from o-suite (right) and e-suite (central) as well as SDS-WAS multi-model product (left) for winter (DJF, top row) and spring (MAM, bottom row). Major dust activity is concentrated over the Sahara (in the Bodelé Basin and the Mali/Mauritania border) and the Arabian Peninsula. From 1 December 2016 to 31 May 2017, e-suite increases the aerosol burden particularly in spring over the main desert dust sources in North Africa and Middle East. Overall, CAMS e-suite increases the dust burden over the study region in comparison with o-suite.

Table 2.1.1: Skill scores (MB, FGE, RMSE and r) of 24h forecasts for CAMS e-suite, CAMS o-suite and SDS-WAS Multi-model Median for the period between 1 December 2016 to 1 June 2017, and the number of data (NDATA) used. Dust filtered AOD (DOD) from AERONET is the reference. CAMS e-suite is the model that best reproduces the DOD AERONET observations (correlation values of 0.79 for o-suite and 0.82 for e-suite and MB of -0.07 for o-suite and -0.06 for e-suite in average for all the AERONET sites). The e-suite results are closer to the SDS-WAS Median Multimodel.

		e-suite				o-suite				SDS-WAS			
	NDATA	MB	FGE	RMSE	r	MB	FGE	RMSE	r	MB	FGE	RMSE	r
Sahara	525	-0.04	0.20	0.24	0.77	-0.07	0.03	0.25	0.76	-0.08	-0.01	0.25	0.77
Sahel	1422	-0.27	-0.49	0.41	0.65	-0.28	-0.52	0.43	0.56	-0.21	-0.32	0.37	0.65
Tropical North Atlantic	226	-0.12	-0.32	0.28	0.71	-0.13	-0.36	0.34	0.53	-0.17	-0.45	0.35	0.54
Subtropical North Atlantic	644	-0.01	0.14	0.11	0.47	-0.01	0.09	0.13	0.40	0.00	0.16	0.14	0.42
North Western Maghreb	275	-0.09	0.01	0.16	0.93	-0.10	-0.03	0.18	0.93	-0.07	0.18	0.15	0.89
Western Iberian Peninsula	793	-0.06	0.27	0.12	0.91	-0.07	0.23	0.13	0.88	-0.06	0.31	0.12	0.88
Iberian Peninsula	1139	-0.03	0.93	0.10	0.82	-0.04	0.92	0.11	0.80	-0.03	0.96	0.11	0.82
Western Mediterranean	3638	-0.02	1.02	0.08	0.75	-0.02	1.01	0.09	0.73	-0.02	1.05	0.08	0.77
Central Mediterranean	3245	-0.02	1.02	0.09	0.86	-0.03	1.00	0.10	0.84	-0.02	1.03	0.09	0.87
Eastern Mediterranean	2468	-0.04	0.93	0.10	0.85	-0.04	0.91	0.11	0.84	-0.03	0.97	0.10	0.83
Eastern Sahara	390	-0.01	0.55	0.13	0.83	-0.03	0.46	0.14	0.82	0.00	0.59	0.13	0.83
Middle East	1504	-0.13	-0.07	0.24	0.72	-0.13	-0.10	0.25	0.67	-0.12	-0.01	0.26	0.66

2.1.3 Mediterranean

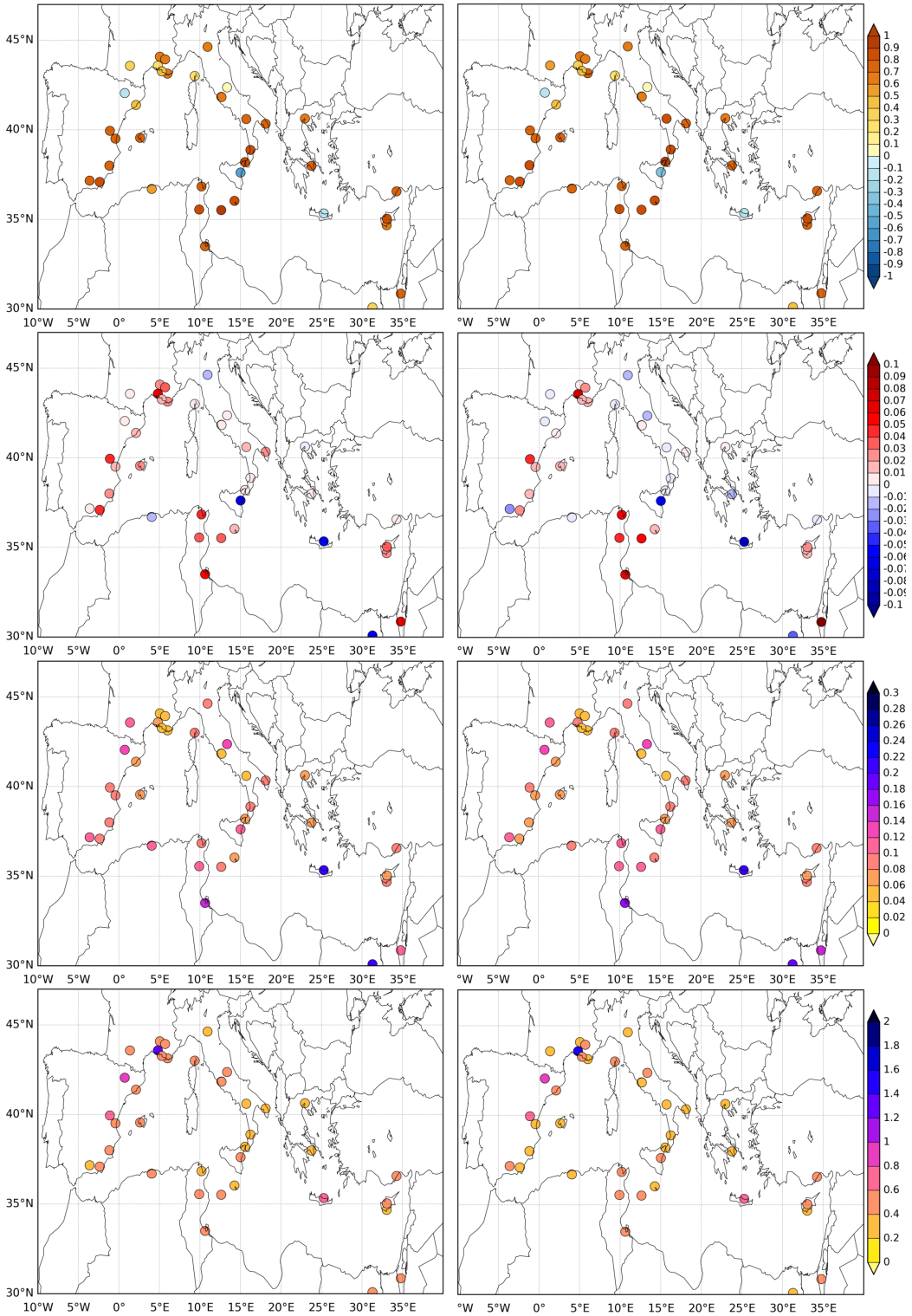

Figure 2.1.7: Skill scores (top row: correlation; second row: mean bias; third row: RMSE; last row: FGE) for 24-hour forecasts of AOD550 CAMS o-suite (left) and e-suite (right) between 1 December 2016 and 1 June 2017. AOD from AERONET Version 3 Level 3 is the reference. Overestimations in Western and Central Mediterranean shown in o-suite are corrected in e-suite with a decrease of MB from 0.02 for o-suite to 0.01 for e-suite.

2.2 Verification of tropospheric ozone

2.2.1 Verification with sonde data in the free troposphere

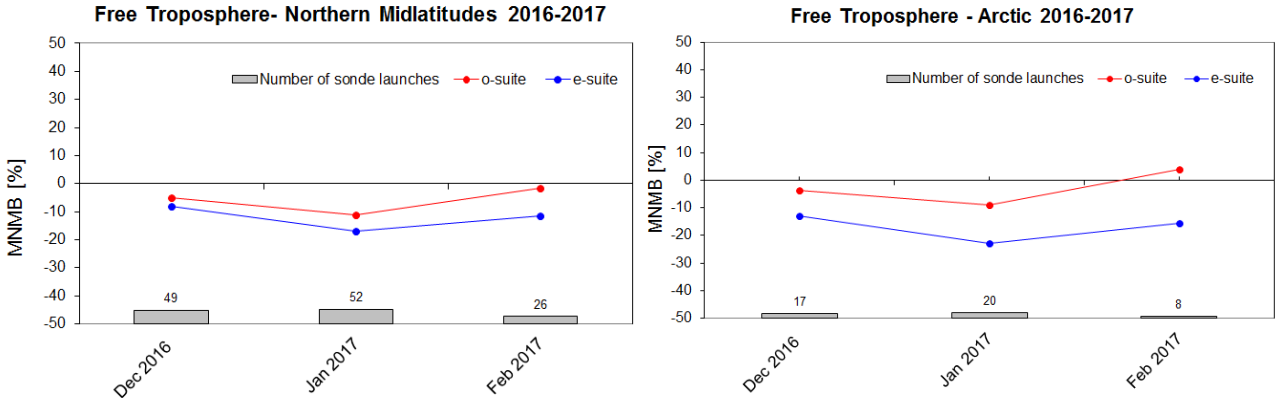

Fig. 2.2.1: MNMBs (%) of ozone in the free troposphere (between 750 and 200 hPa (Tropics) / 300 hPa) from the IFS model runs against aggregated sonde data over the Northern midlatiutdes (left) and the Arctic (right). The numbers indicate the amount of individual number of sondes.

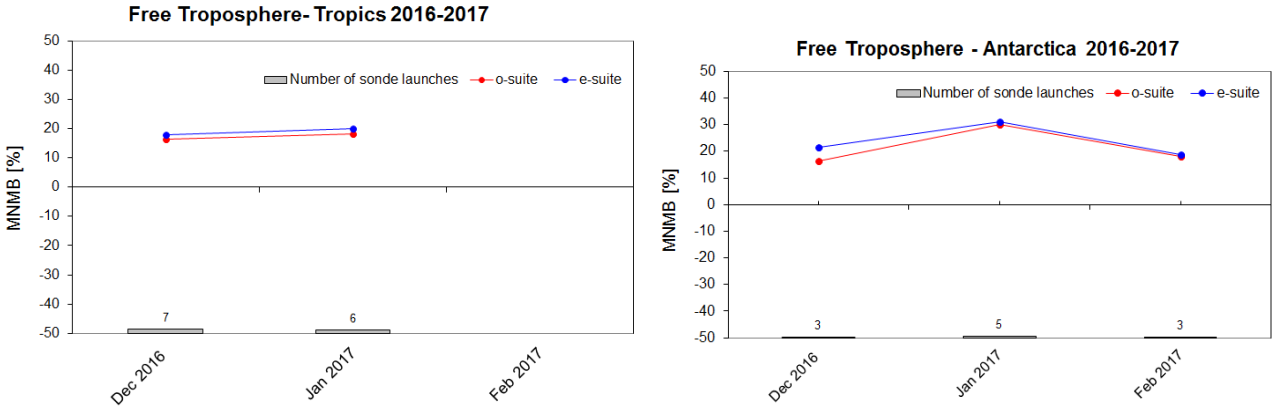

Fig. 2.2.2: MNMBs (%) of ozone in the free troposphere (between 750 and 200 hPa (Tropics) / 300 hPa) from the IFS model runs against aggregated sonde data over the Tropics (left) and Antarctica (right). The numbers indicate the amount of individual number of sondes.

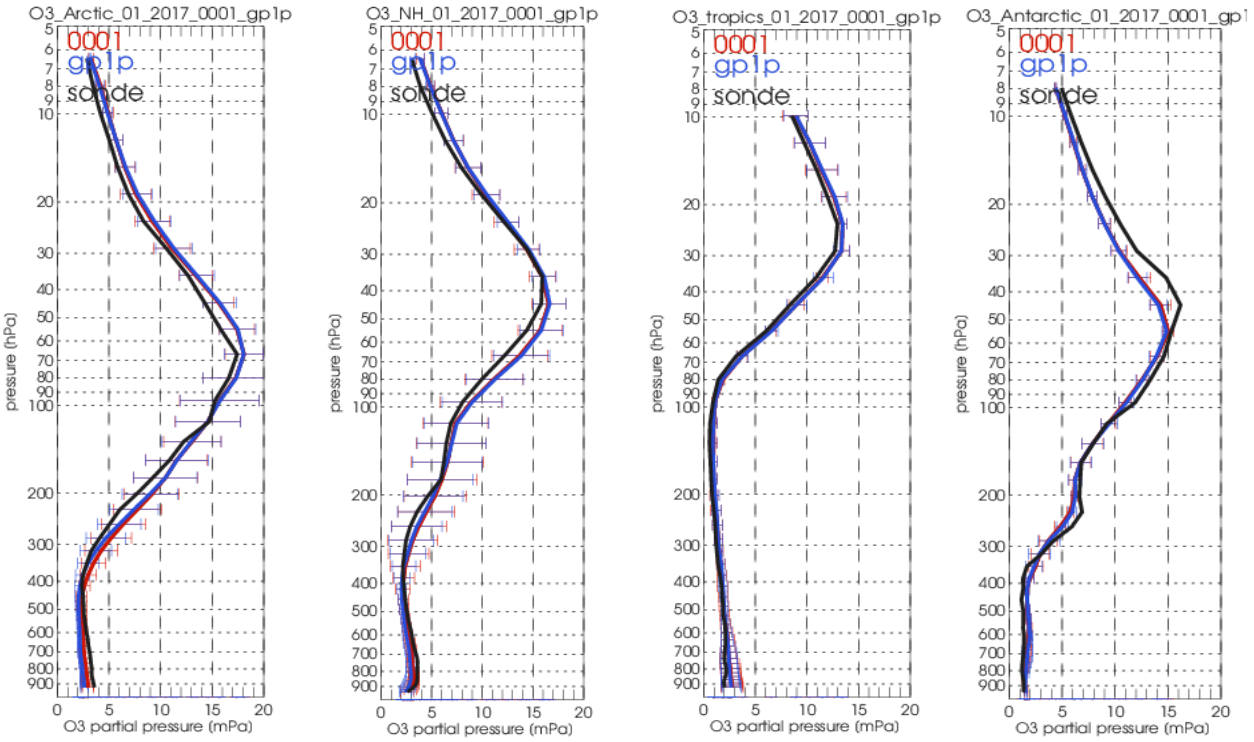

Fig. 2.2.3: Ozone sonde profiles over the Arctic (left), Nothern Midlatitudes (mid-left), Tropics (mid-right) and Antarctica (right) for January 2017.

2.2.2 Verification with GAW and ESRL-GMD surface observations

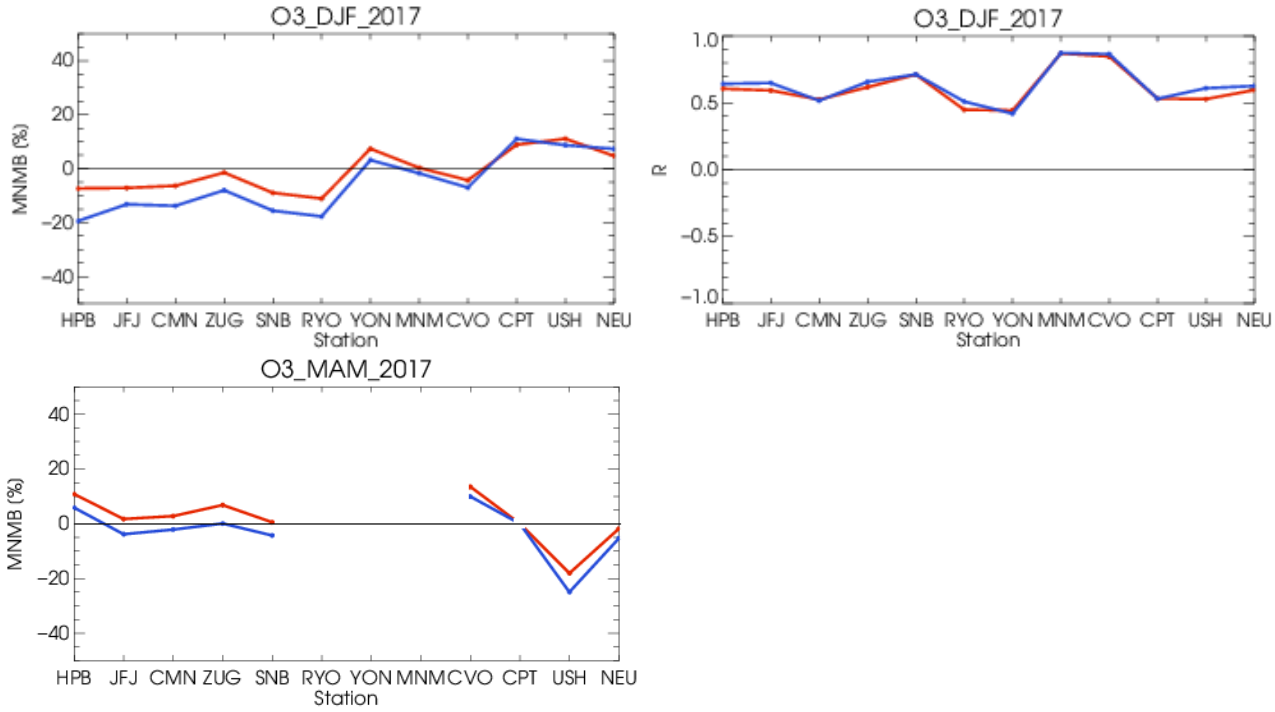

Fig. 2.2.4: MNMB [%] (left) and R (right) for the evaluation of modelled O3 surface mixing ratios with observations of 12 GAW stations. Bottom: MNMB for March-May 2017. The difference between o-suite and e-suite increases towards higher latitudes. For MAM the e-suite is still somewhat lower at the GAW stations, which in part represents an improvement in terms of bias.

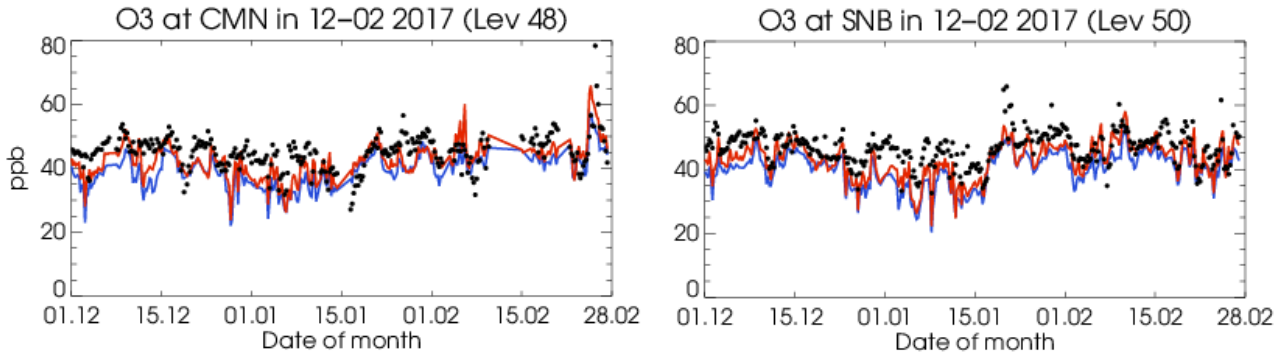

Fig. 2.2.5: Time series of ozone volume mixing ratio (ppbv) for the o-suite (red) and e-quite (blue) compared to GAW observations at Monte Cimone(left) and Sonnblick (right).

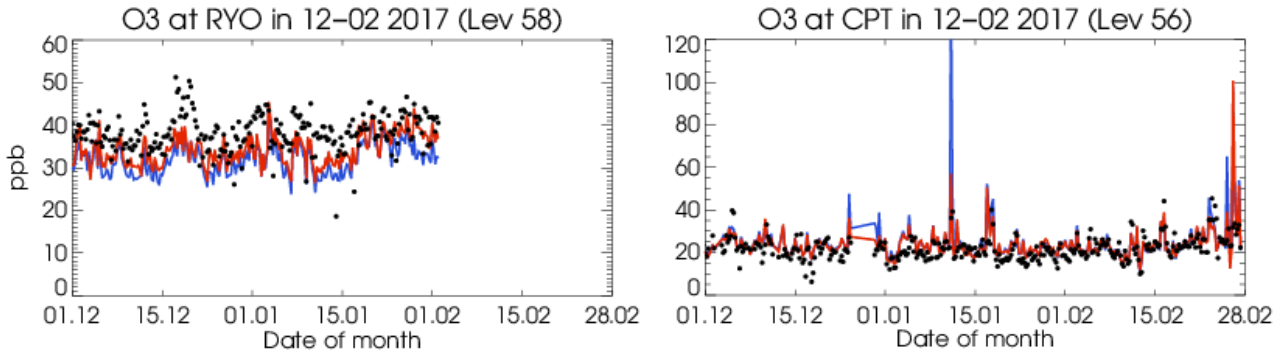

Fig. 2.2.6: Time series of ozone volume mixing ratio (ppbv) for the o-suite (red) and e-quite (blue) compared to GAW observations at Ryori (left) and Cape Point (right).

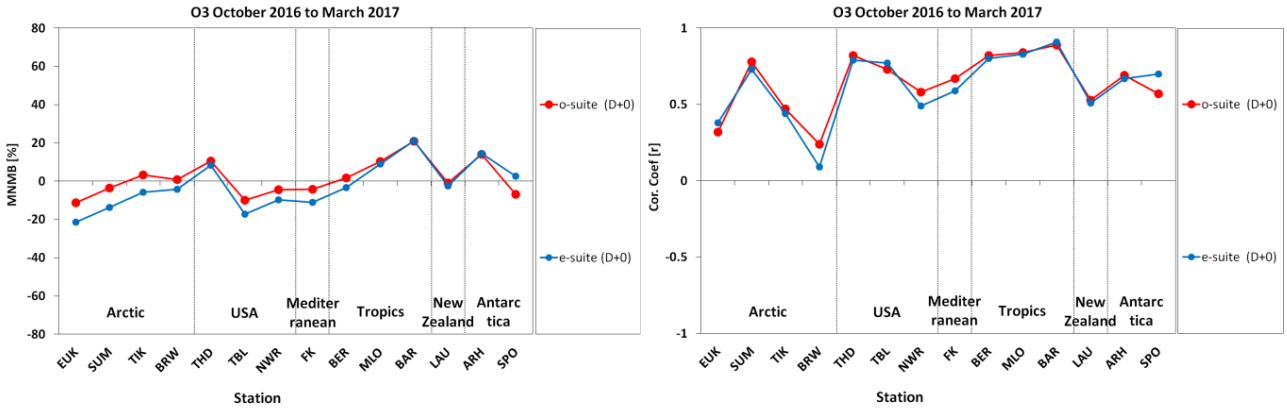

Fig. 2.2.7: MNMB [%] (left) and R (right) for the evaluation of modelled O3 surface mixing ratios with observations of 13 ESRL stations Period: October 2016 - March 2017.

Table 2.2.1: Averaged Biases, MNMBs and correlations coefficients from the evaluation of the e-suite and o-suite against ESRL observations for the period 10/2016 to 03/2017.

	Arctic				USA			Mediterranean	Tropics			New Zeanland	Antarctica	
	EUK	SUM	TIK	BRW	THD	TBL	NWR	FK	BMW	MLO	RPB	LAU	ARH	SPO
Lat	80.05	72.57	71.60	71.32	41.05	40.12	40.04	35.32	32.27	19.54	13.17	-45.04	-77.80	-90.00
Lon	-86.42	-38.38	128.90	-156.61	-124.15	-105.24	-105.54	25.67	-64.88	-155.58	-59.46	169.68	-166.78	-24.80
Alt	610	3266	250	8	107	1689	3022	250	30	3397	45	370	50	2837
o-suite Bias (ppb)	-4.0	-1.1	1.0	-0.4	3.4	-2.8	-1.6	-1.6	0.3	3.8	4.9	0.2	3.0	-2.2
e-suite Bias (ppb)	-7.6	-5.1	-1.7	-2.1	2.5	-5.3	-3.8	-4.2	-1.9	3.0	4.7	0.0	3.1	0.6
o-suite MNMB [%]	-11.2	-3.5	3.3	0.8	10.5	-10.0	-4.4	-4.2	1.8	10.4	20.9	-1.0	14.1	-6.9
e-suite MNMB [%]	-21.5	-13.7	-5.7	-4.3	8.3	-17.2	-9.7	-11.1	-3.4	9.0	21.1	-2.4	14.6	2.6
o-suite R	0.32	0.78	0.47	0.24	0.82	0.73	0.58	0.67	0.82	0.84	0.89	0.53	0.69	0.57
e-suite R	0.38	0.73	0.44	0.09	0.79	0.77	0.49	0.59	0.80	0.83	0.91	0.51	0.67	0.70

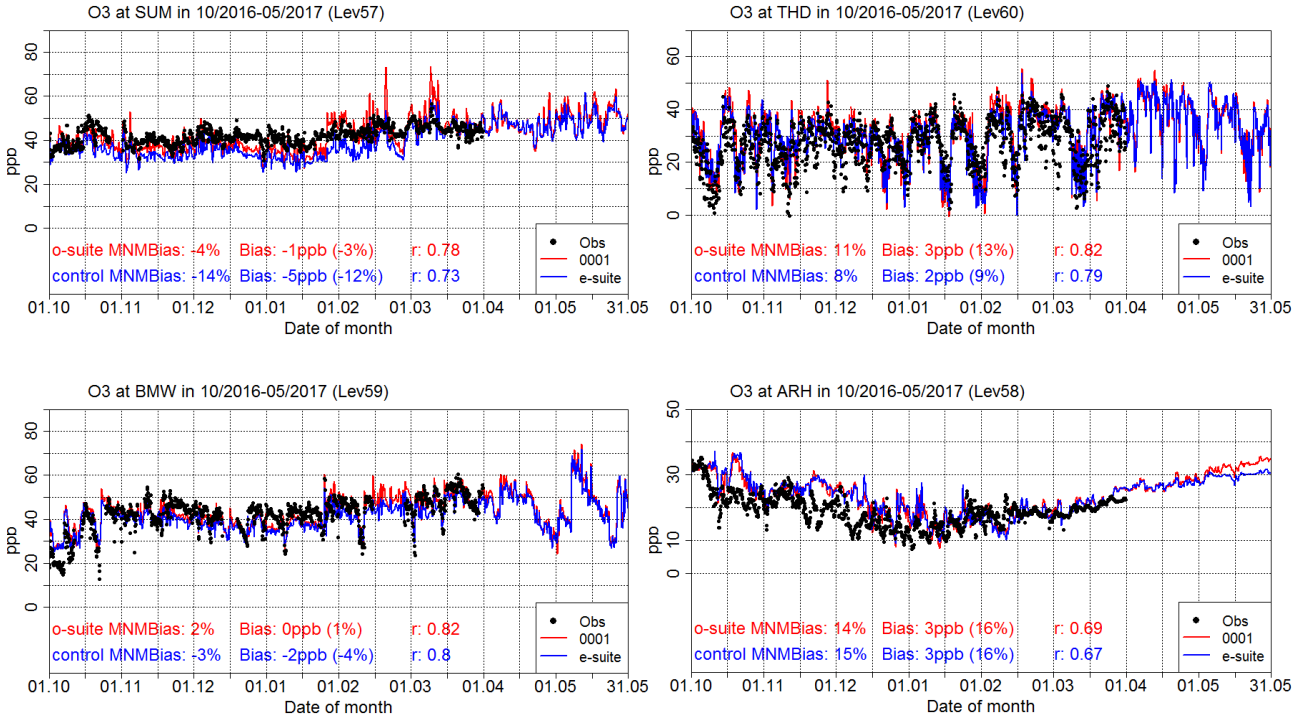

Fig. 2.2.8: Time series of ozone volume mixing ratio (ppbv) for the o-suite (red) and e-suite (blue) compared to ESRL observations at Summit, Greenland (72.57°N, 38.48°W, upper left), Trinidad Head, USA (41.05°N, 124.15°W upper right), at Tudor Hill, Bermuda (32.27°N, 64.88°W, lower left right), and Arrival Heights, Antarctica (77.83°S, 166.20°E, lower right)

2.2.3 Verification with IAGOS ozone observations

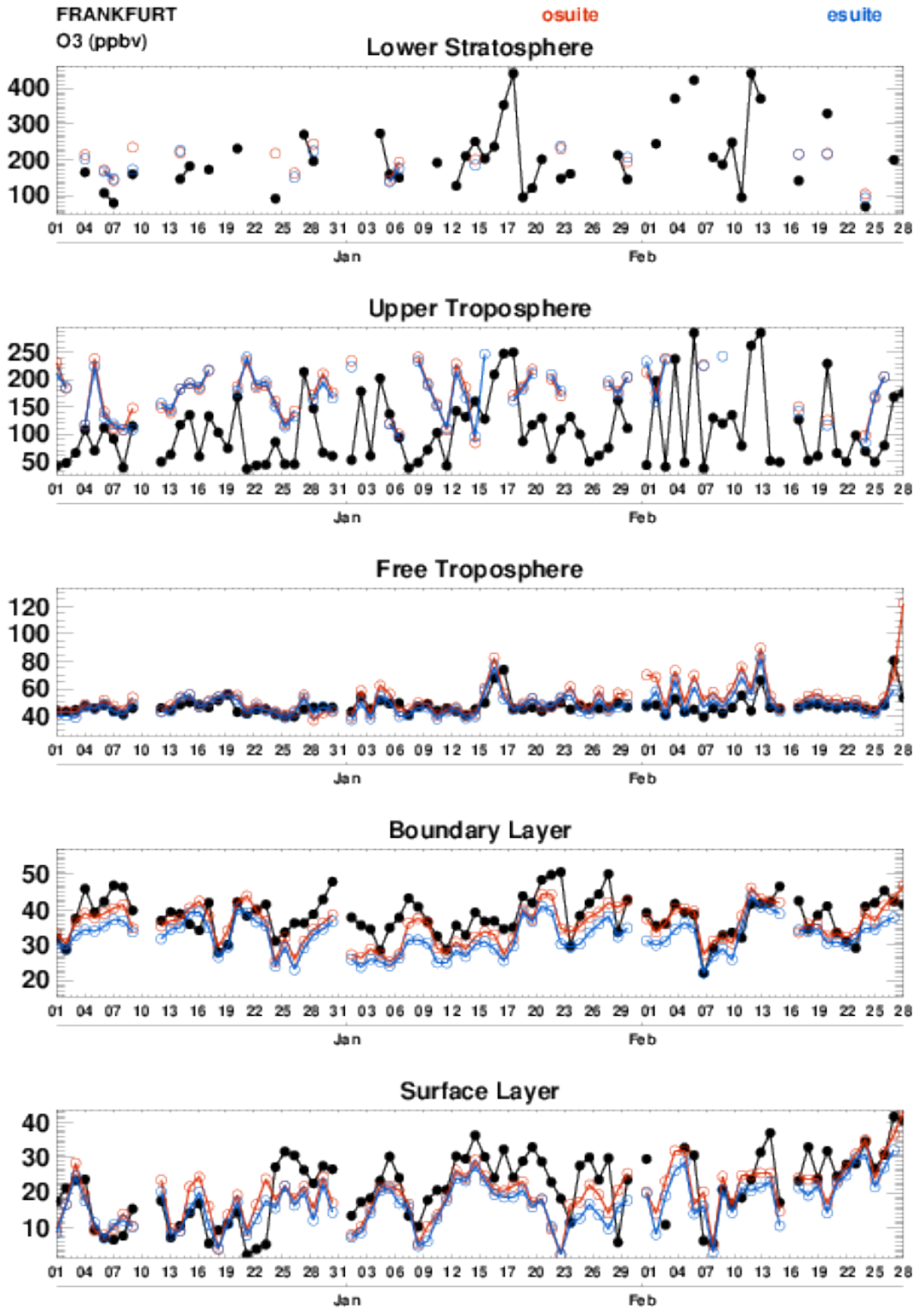

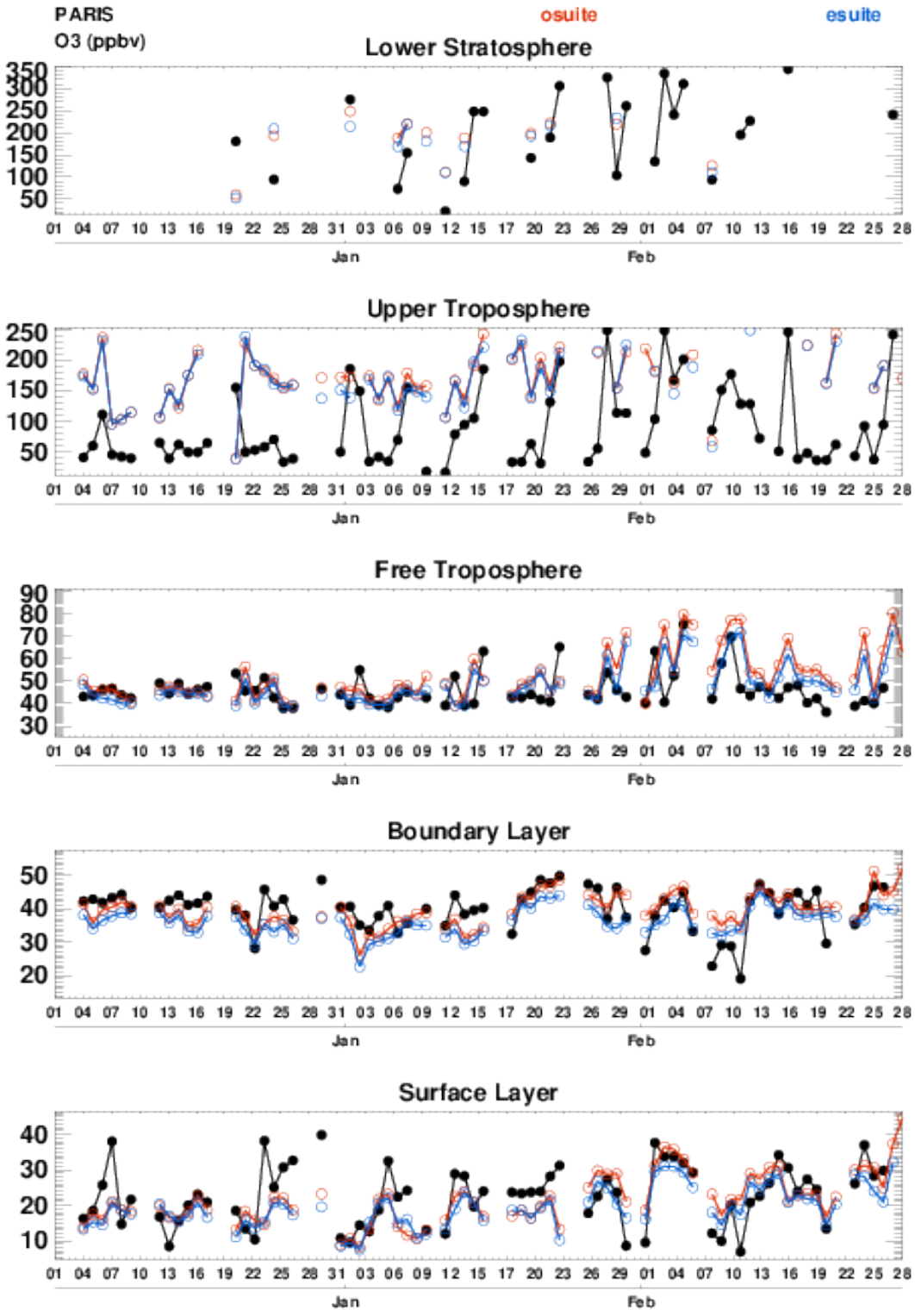
PARIS
O3 (ppbv)
osuite
esuite
Lower Stratosphere
Upper Troposphere
Free Troposphere
Boundary Layer
Surface Layer
Jan
Feb

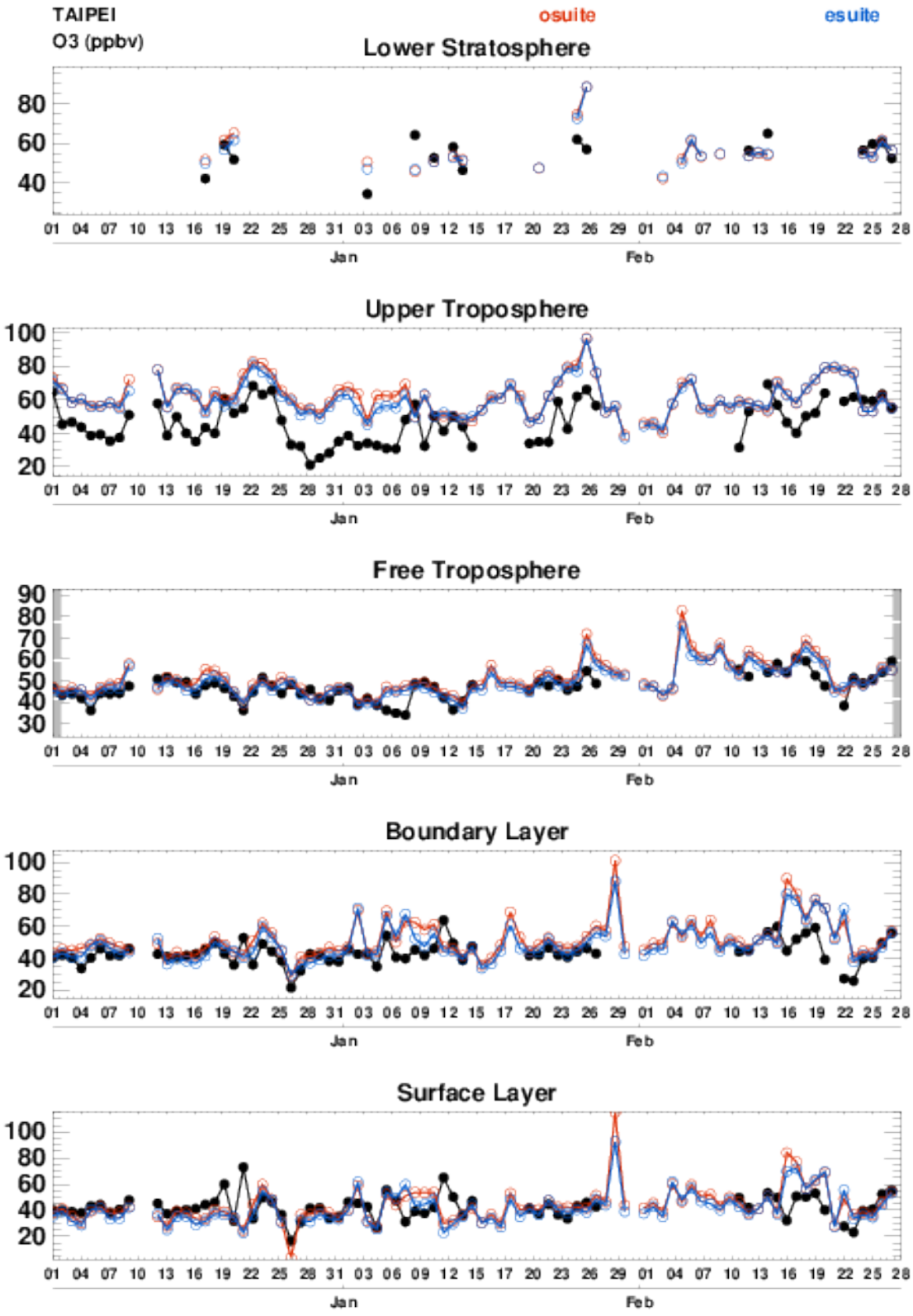

Figure 2.2.9: Timeseries of ozone over Frankfurt, Paris and Taipei from December 2016-February 2017.

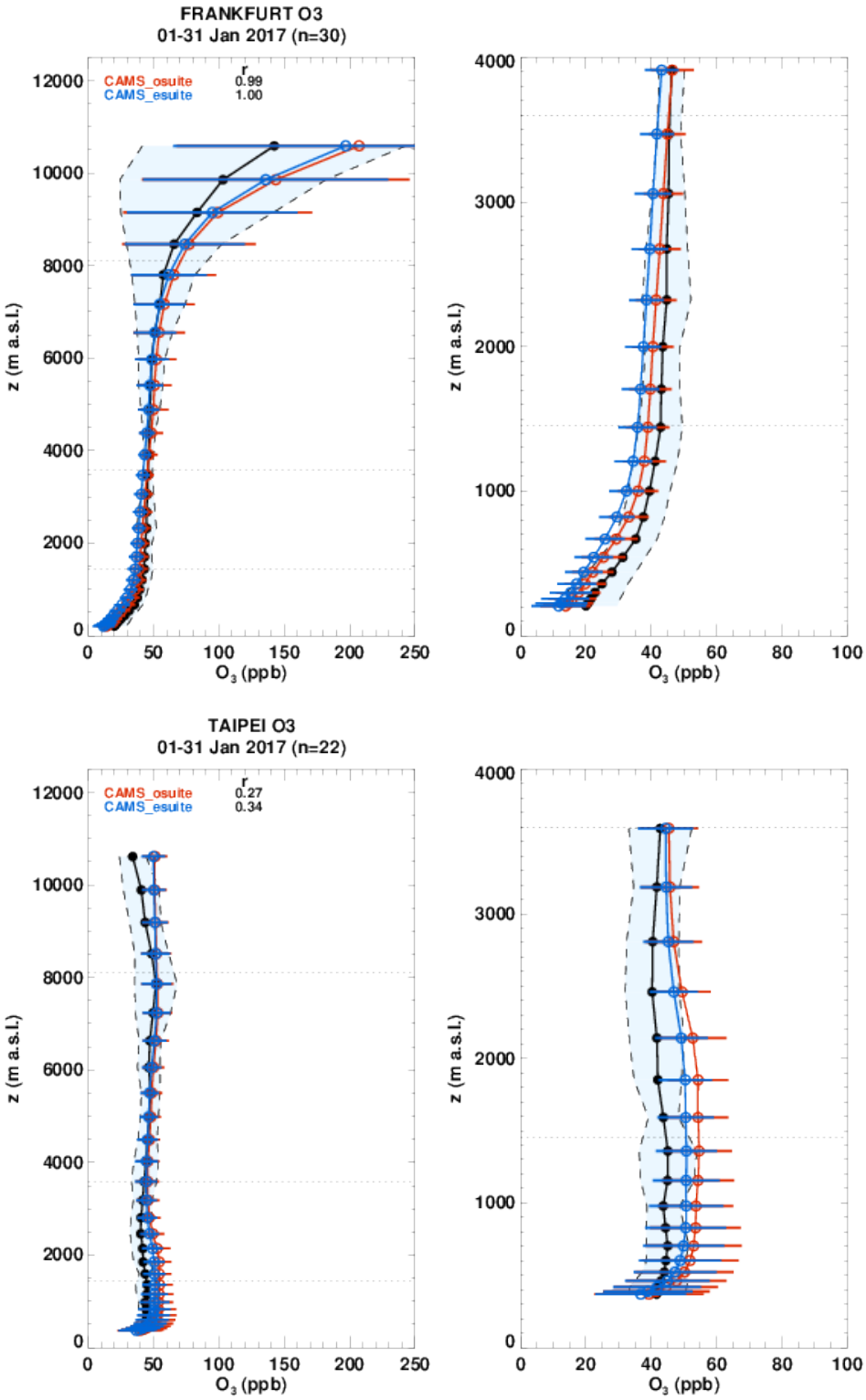

Figure 2.2.10: Profiles of ozone over Frankfurt and Taipei in January 2017.

2.2.4 Verification of ozone in the Mediterranean

Table 2.2.2: Coordinates, elevation, corresponding model level (level 60 is the surface level), as well as validation scores (Biases, MNMBs and correlations for the period 10/2016-05/2017) obtained with the 2 forecast runs (o-suite and e-suite), for each one of the selected Mediterranean stations. Biases, MNMBs and correlations with blue denote stations where e-suite performs better while with red are denoted stations where o-suite performs better. The surface ozone validation analysis over the Mediterranean is based on an evaluation against station observations from the Airbase Network (http://acm.eionet.europa.eu/databases/airbase/). In addition, 3 stations from the Department of Labour Inspection - Ministry of Labour and Social Insurance, of Cyprus (http://www.airquality.dli.mlsi.gov.cy/) as well as the Navarino Environmental Observatory (http://www.navarinoneo.gr/index.php/en/) station in Messene Greece are used in the validation analysis. For the validation analysis, stations in the Mediterranean located within about 100 km from the shoreline of the Mediterranean shore are used.

						Distance from the	Bias (ppb)		MNMB [%]		Cor. Coef	
Station Name	Stat_ID	Lon	Lat	Alt (m)	Level	shore (km)	o-suite	e-suite	o-suite	e-suite	o-suite	e-suite
Al Cornocales	ES1648A	-5.66	36.23	189	57	16	6.0	3.9	15.7	10.5	0.69	0.67
Caravaka	ES1882A	-1.87	38.12	1	60	73	-8.6	-10.3	-27.6	-33.4	0.76	0.77
Zarra	ES0012R	-1.10	39.08	885	56	70	-2.9	-4.6	-7.9	-11.9	0.78	0.75
Vlillar Del Arzobispo	ES1671A	-0.83	39.71	430	60	48	-4.3	-6.0	-15.5	-20.7	0.79	0.80
Cirat	ES1689A	-0.47	40.05	466	60	37	0.9	-0.3	3.9	0.7	0.77	0.77
Bujaraloz	ES1400A	-0.15	41.51	327	60	60	-6.3	-8.0	-34.8	-41.0	0.74	0.73
Morella	ES1441A	-0.09	40.64	1150	53	51	-0.2	-2.6	-0.5	-6.5	0.85	0.86
Bc-La Senia	ES1754A	0.29	40.64	428	59	21	-4.1	-6.1	-13.2	-19.4	0.70	0.68
Ay-Gandesa	ES1379A	0.44	41.06	368	58	15	3.4	1.3	11.3	6.0	0.86	0.83
Ak-Pardines	ES1310A	2.21	42.31	1226	57	81	7.5	5.0	18.6	12.8	0.41	0.42
Hospital Joan March	ES1827A	2.69	39.68	172	57	3	6.1	3.9	12.3	7.2	0.67	0.66
Al-Agullana	ES1201A	2.84	42.39	214	60	25	-5.3	-7.2	-23.4	-30.8	0.66	0.65
Av-Begur	ES1311A	3.21	41.96	200	56	9	0.9	-1.4	0.1	-5.6	0.81	0.82
Plan Aups/Ste Baume	FR03027	5.73	43.34	675	54	21	3.9	0.6	8.5	0.3	0.76	0.75
Gharb	MT00007	14.20	36.07	114	57	31	0.9	-0.9	1.7	-2.4	0.75	0.73
Aliartos	GR0001R	23.11	38.37	110	59	18	-2.3	-4.7	-1.0	-8.7	0.70	0.75
NEO	-	21.67	37.00	50	60	2	2.8	0.2	7.9	0.7	0.67	0.69
Finokalia	GR0002R	25.67	35.32	250	57	4	-1.6	-4.2	-4.2	-11.1	0.67	0.59
Ineia	-	32.37	34.96	672	52	5	-1.8	-3.6	-4.0	-8.4	0.79	0.80
Oros Troodos	-	32.86	34.95	1819	49	11	2.3	-0.5	4.0	1.3	0.80	0.82
Agia Marina	CY0002R	33.06	35.04	532	55	14	3.4	1.2	6.3	1.8	0.74	0.74

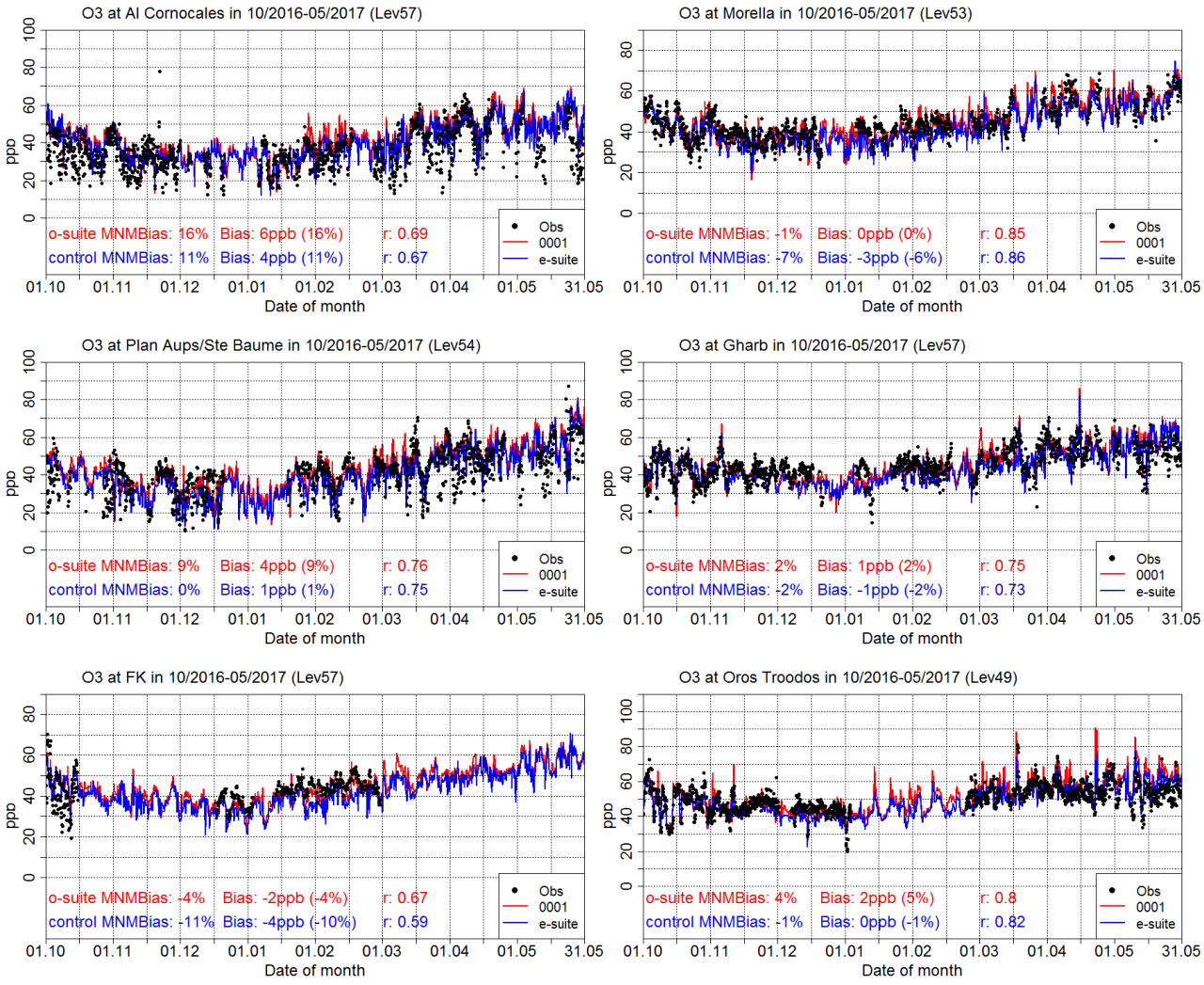

Fig. 2.2.11: Time series of ozone volume mixing ratio (ppbv) for the o-suite (red) and e-suite(blue) compared to AirBase observations at Al Cornocales, Spain(36.23°N, 5.66°W, upper left), Morella, Spain(40.64°N, 0.09°W,upper right), Plan Aups/Ste Baume, France (43.34°N, 5.73°E, middle left), Gharb, Malta (36.07°N, 14.20°E, middle right), Finokalia, Crete station (35.32°N, 25.67°E, lower left) and Mountain Troodos, Cyprus (34.95°N, 32.86°E, lower right).

2.2.5 Verification with ozone surface data in the Arctic

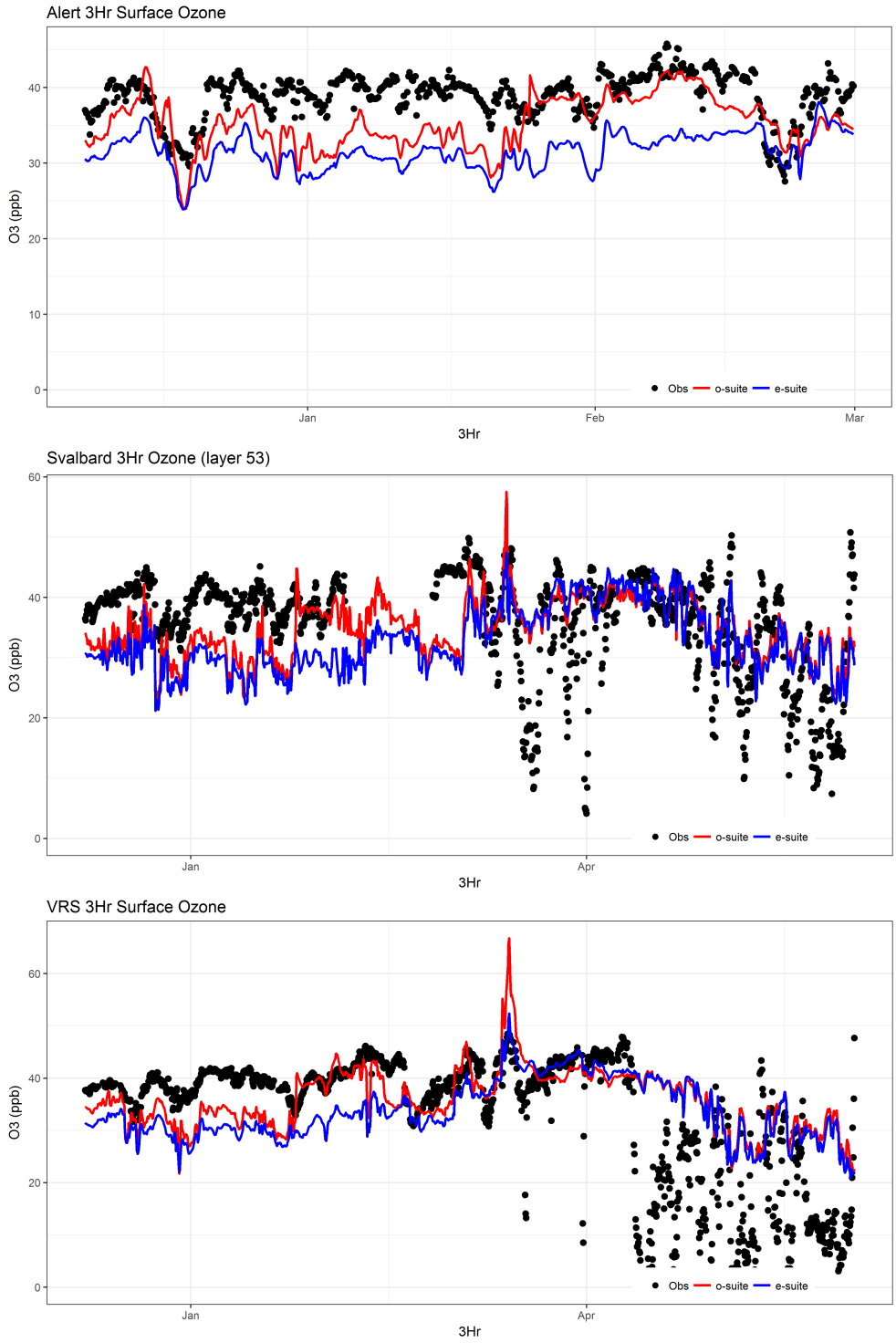

Fig. 2.2.12: Surface ozone concentrations at Alert, Canada (top) from December 2016 – February 2017 and for the Zeppelin Mountain, Svalbard (middle) and Villum Research Station, Greenland (bottom) from December 2016 – May 2017. Before 24 January the previous o-suite and e-suite are similar but the o-suite is a bit lower. In late January and early February the current o-suite is higher than the e-suite and fits the data better. From the end of February onwards the currrent o-suite and e-suite are very similar in the Arctic.

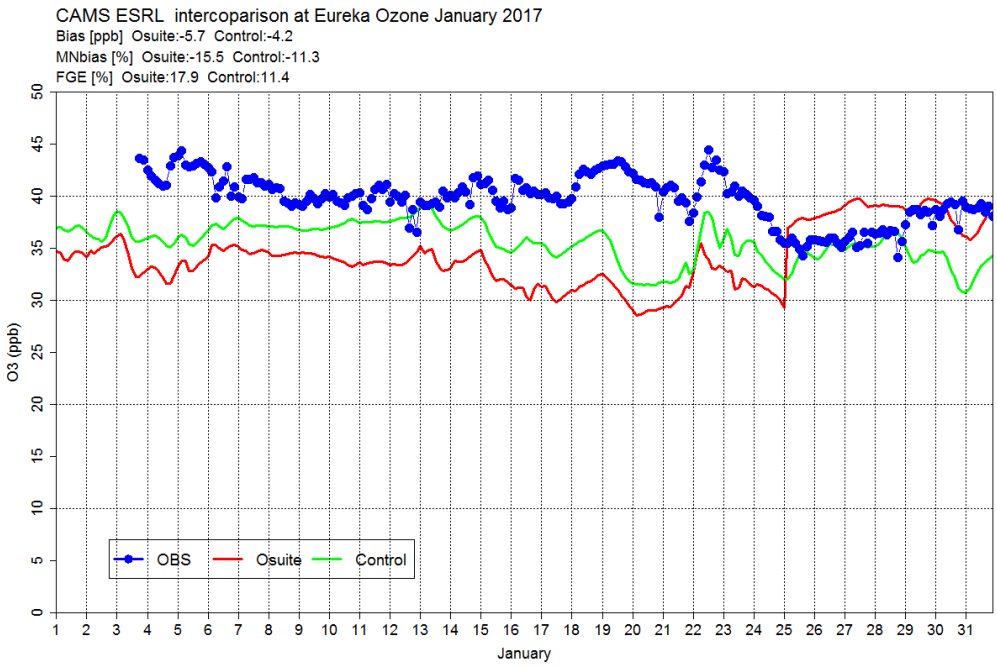

Fig. 2.2.13: Surface ozone concentrations at Eureka, Canada, 80 N, for January 2017. The jump in ozone in the o-suite on 24 January is clearly visible, but is absent in the corresponding control run without data assimilation (green line), suggesting that the changes between the two o-suite versions are related to the assimilation.

2.3 Carbon monoxide

2.3.1 Validation with Global Atmosphere Watch (GAW) Surface Observations

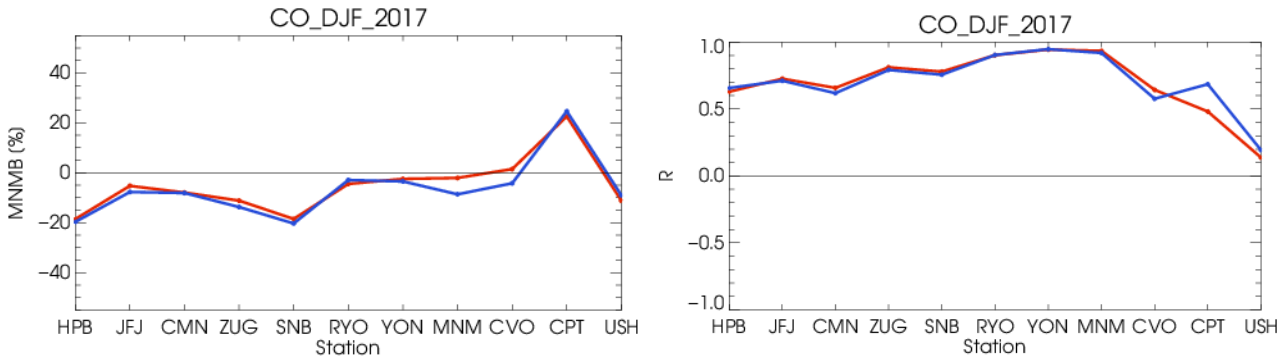

Fig. 2.3.1: MNMB [%] (left) and R (right) for the evaluation of modelled CO surface mixing ratios with observations of 11 GAW stations

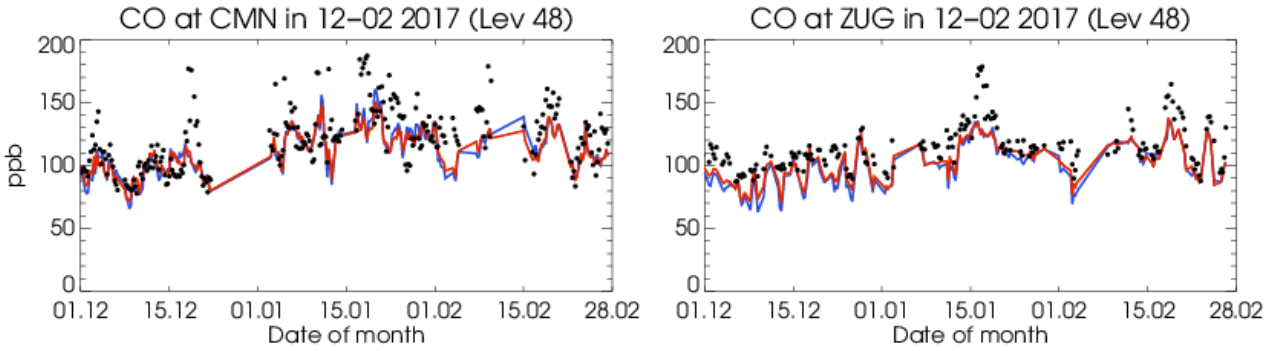

Fig. 2.3.2: Time series of carbon monoxide volume mixing ratio (ppbv) for the o-suite (red) and e-quite (blue) compared to GAW observations at Monte Cimone (left) and Zugspitze (right).

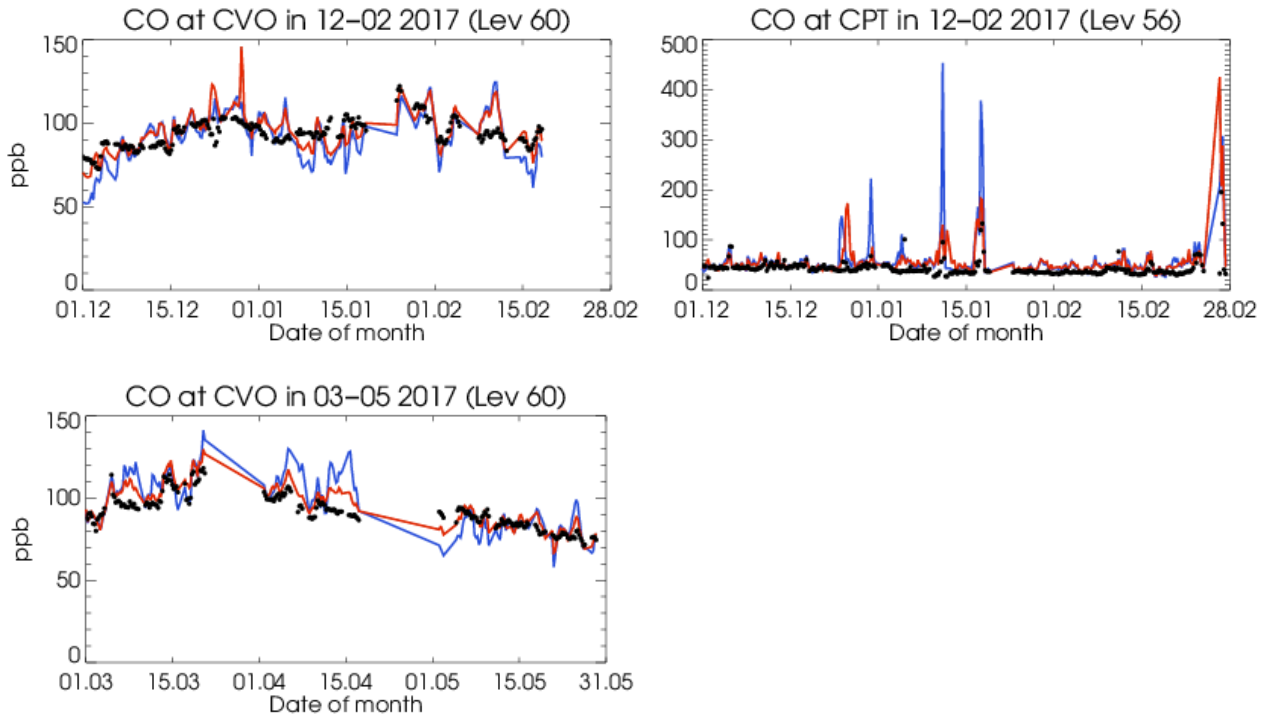

Fig. 2.3.3: Time series of carbon monoxide volume mixing ratio (ppbv) for DJF-2017 for the o-suite (red) and e-quite (blue) compared to GAW observations at Cape Verde (left) and Cape Point (right). Bottom: time series at Cape Verde for MAM-2017.

2.3.2 IAGOS Aircraft observations

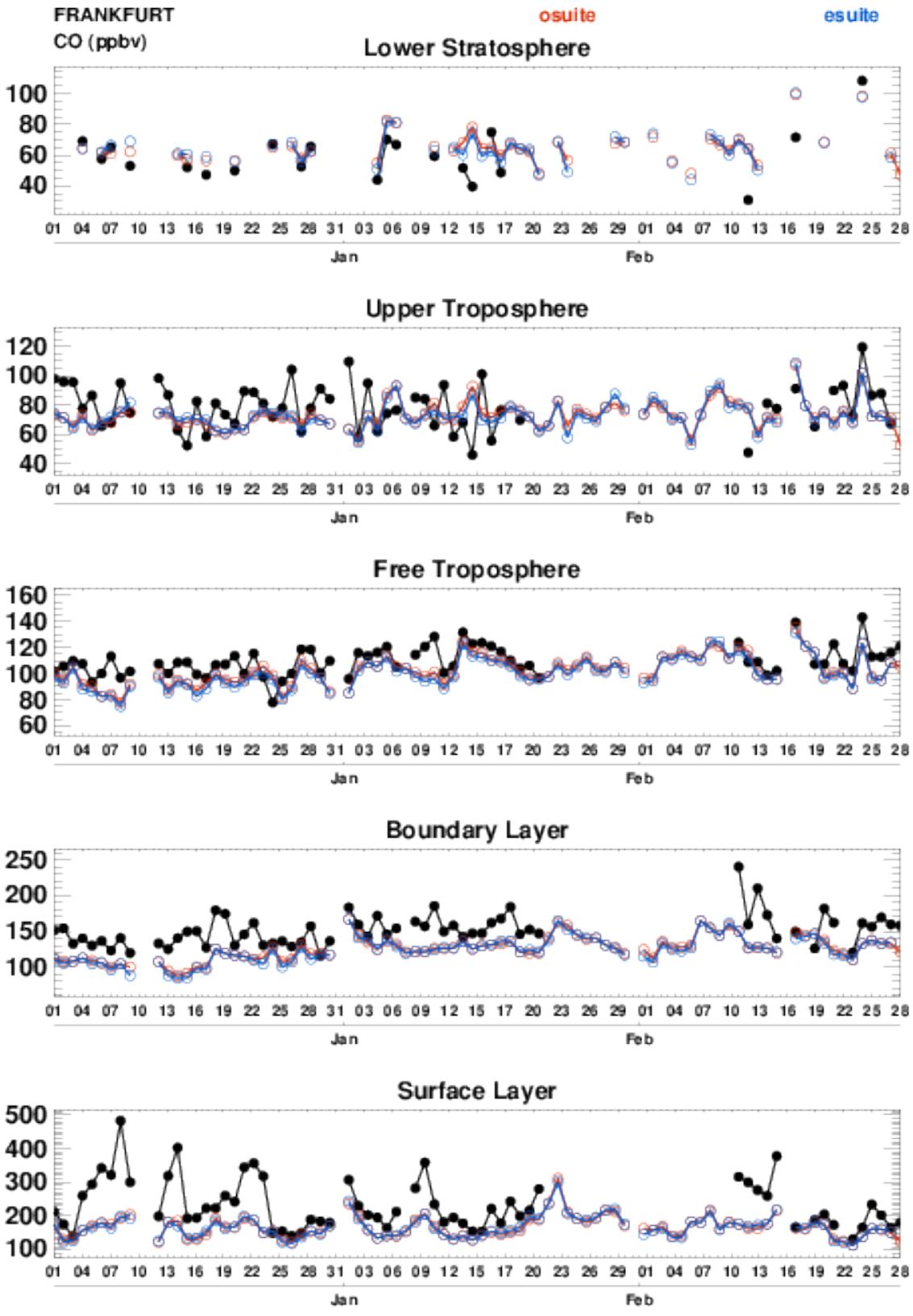

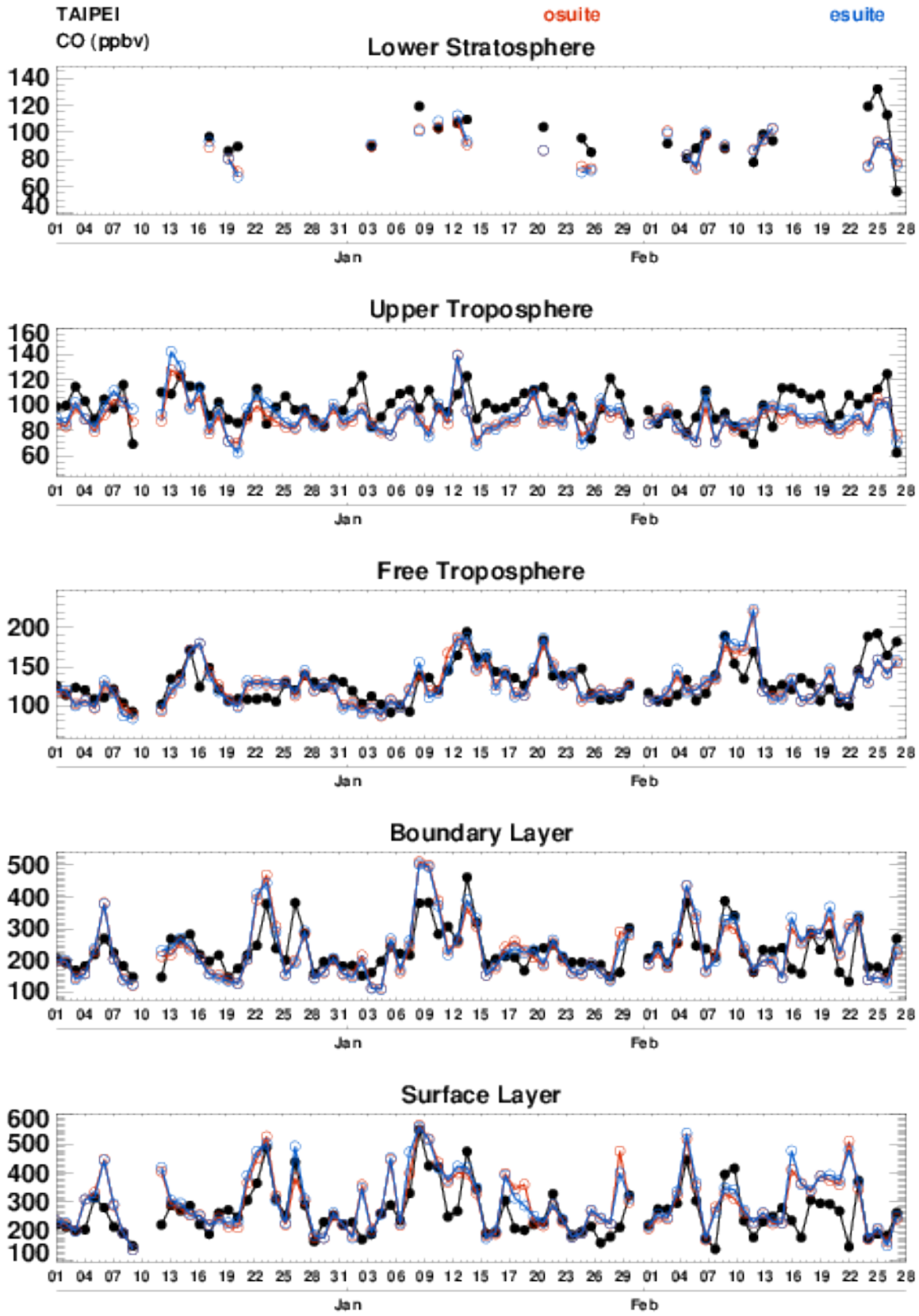

Figure 2.3.4: Timeseries of carbon monoxide over Frankfurt and Taipei from December-February 2016/17.

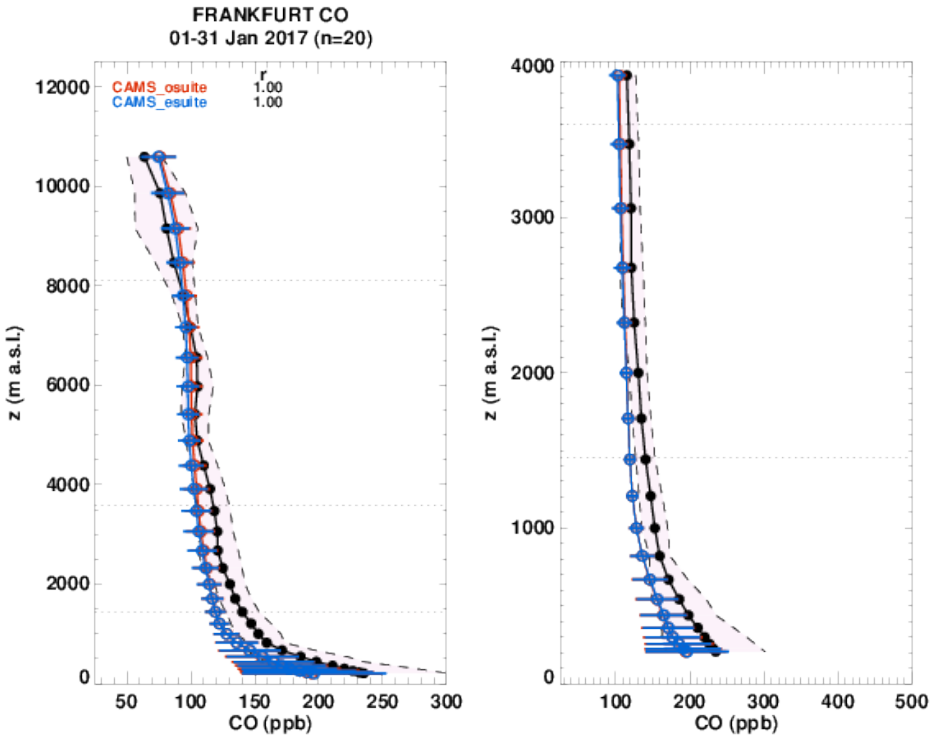

Figure 2.3.5 : Profile of carbon monoxide over Frankfurt for January 2017.

2.3.3 FTIR CO observations

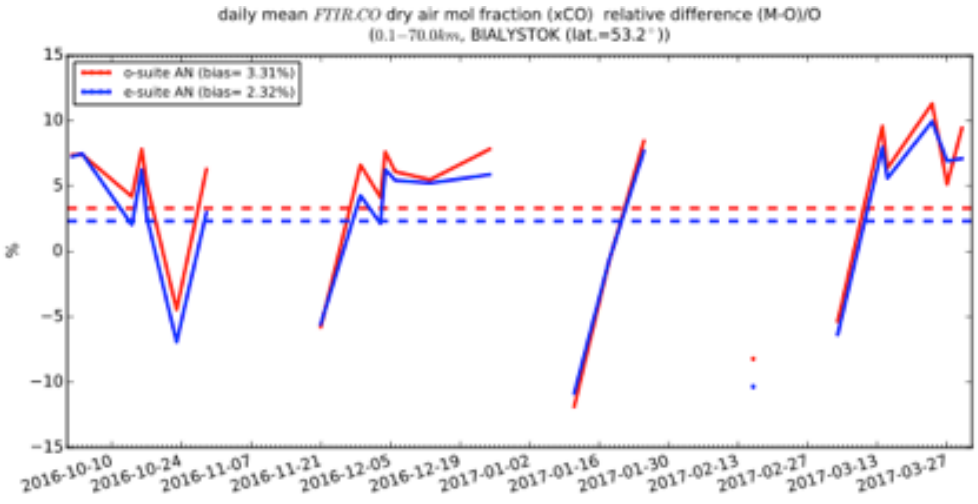

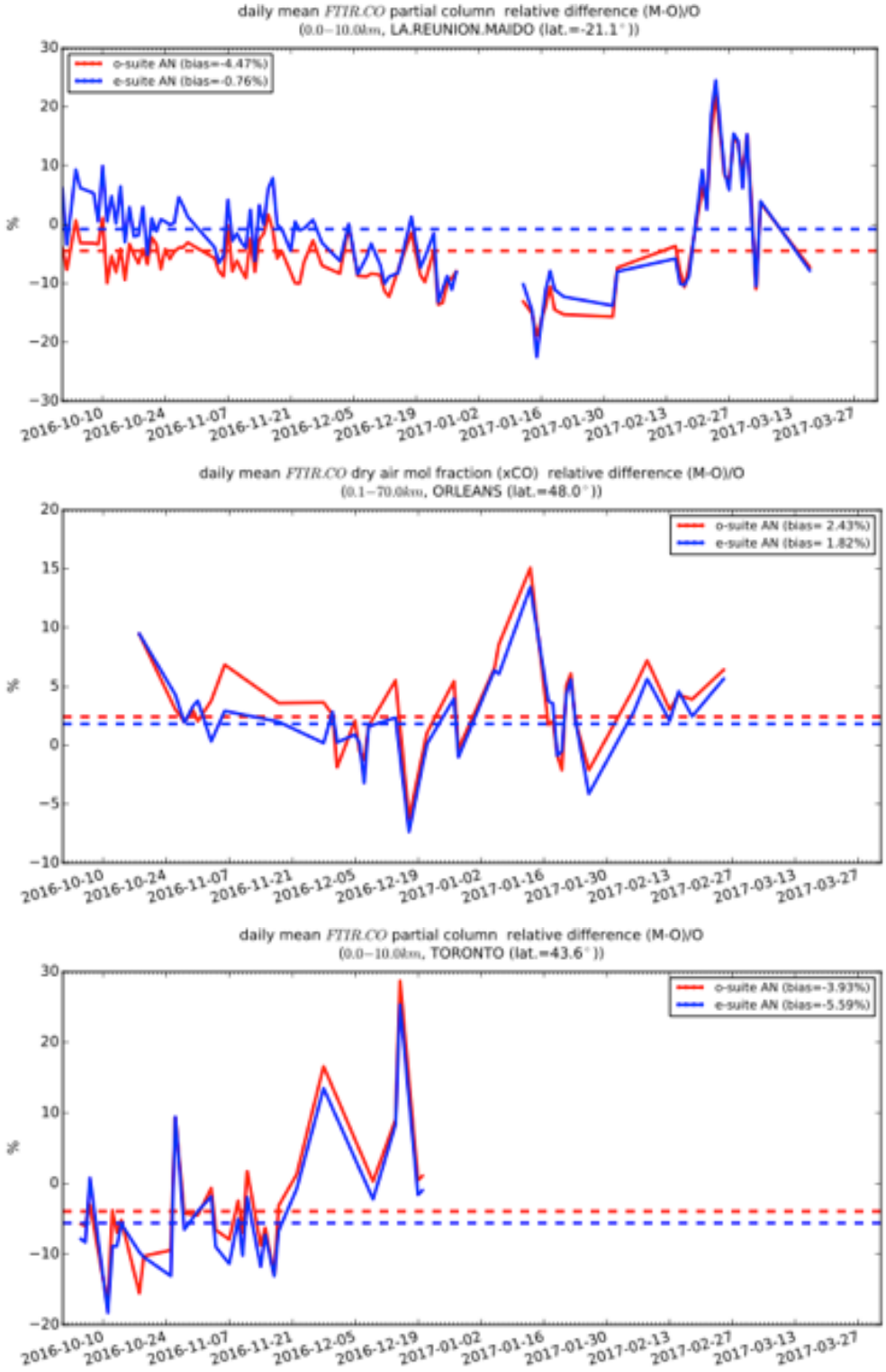

Fig. 2.3.6.: Comparison of daily mean bias between the o- and e-suite CO partial column for the TCCON stations Bialystok and Orleans and the NDACC stations at Reunion and Toronto. The performance of the e-suite depends on the site.

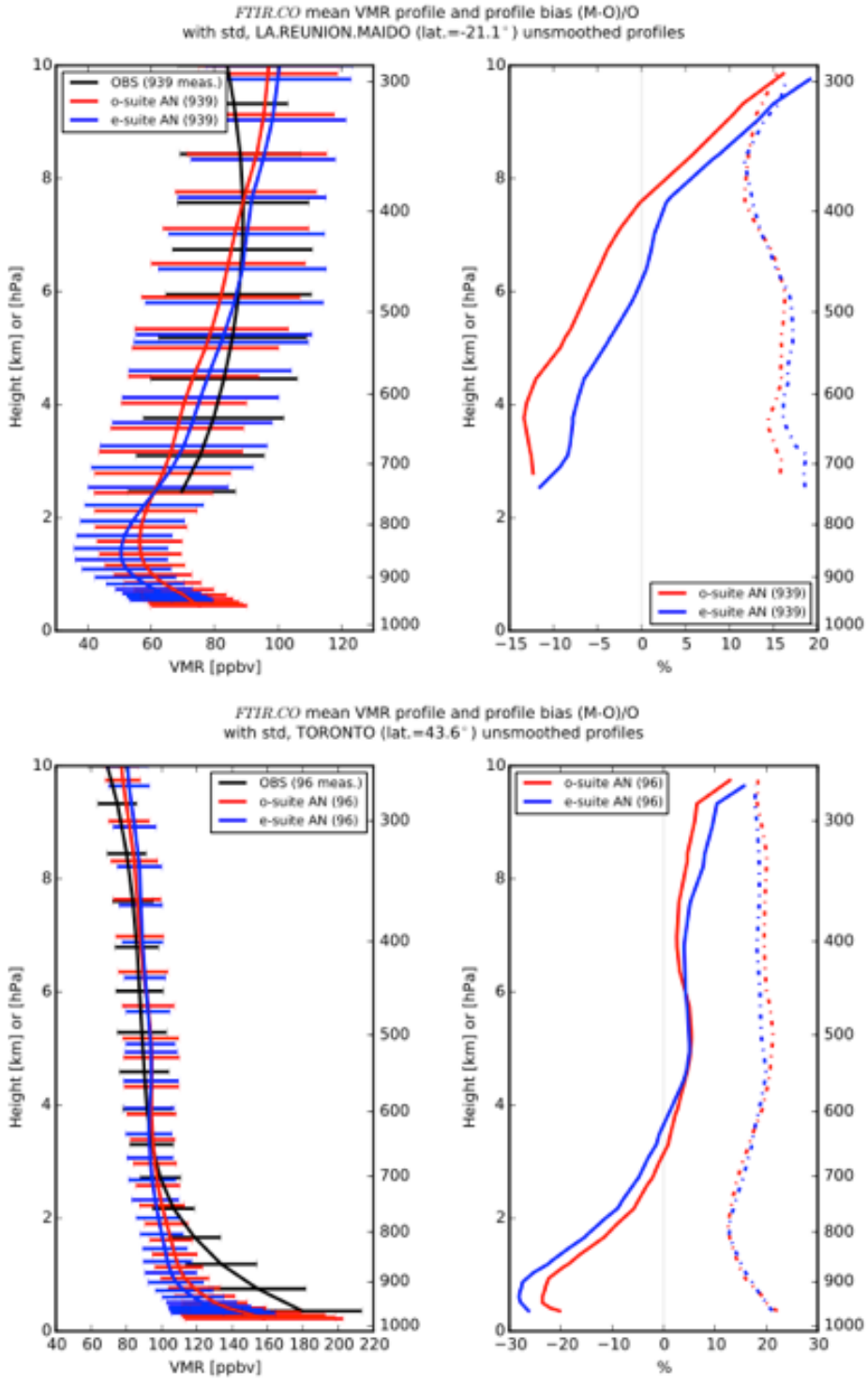

Fig. 2.3.7: Averaged profile comparison and relative profile bias between the o-suite and e-suite CO tropospheric profile for the NDACC stations at Reunion and Toronto (right) Oct 2016 - March 2017. The performance of the e-suite depends on the site.

2.3.4 Comparisons with MOPITTv6 and IASI CO data

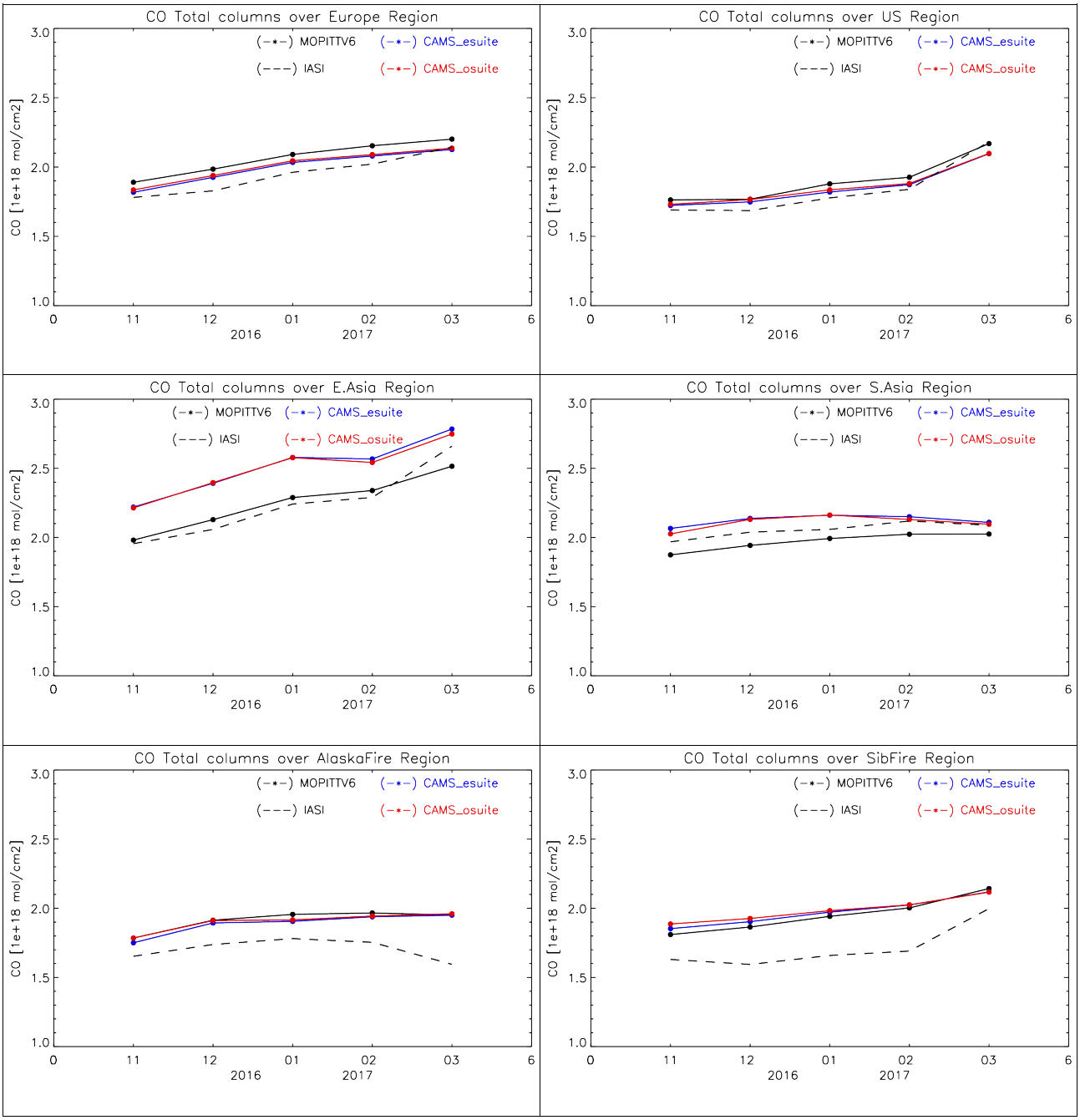

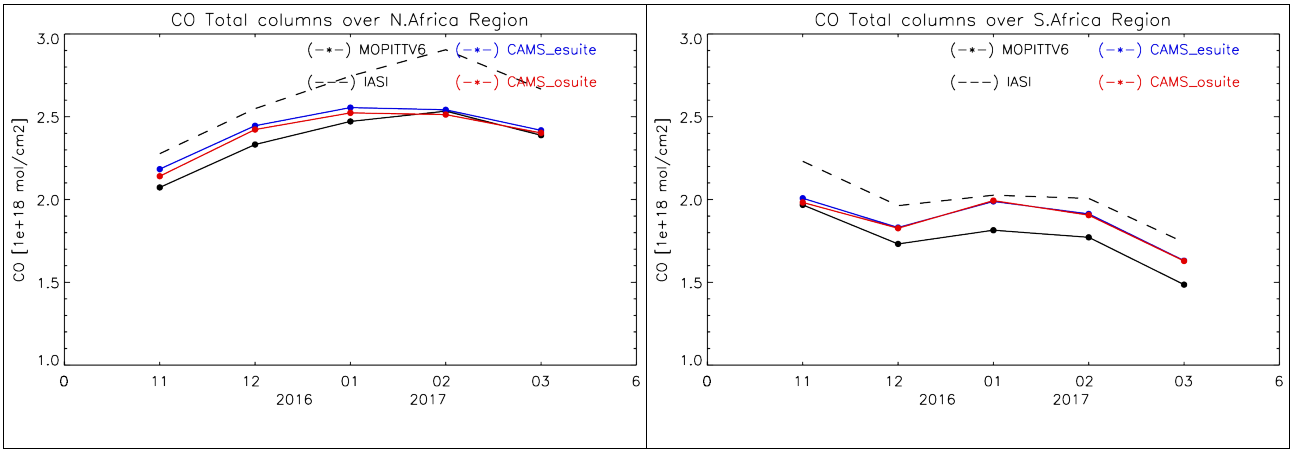

Fig.2.3.8 Time series of CO total columns for MOPITT v6 and IASI and the model simulations o-suite (red) and e-suite (blue) over selected regions for November 2016 until March 2017.

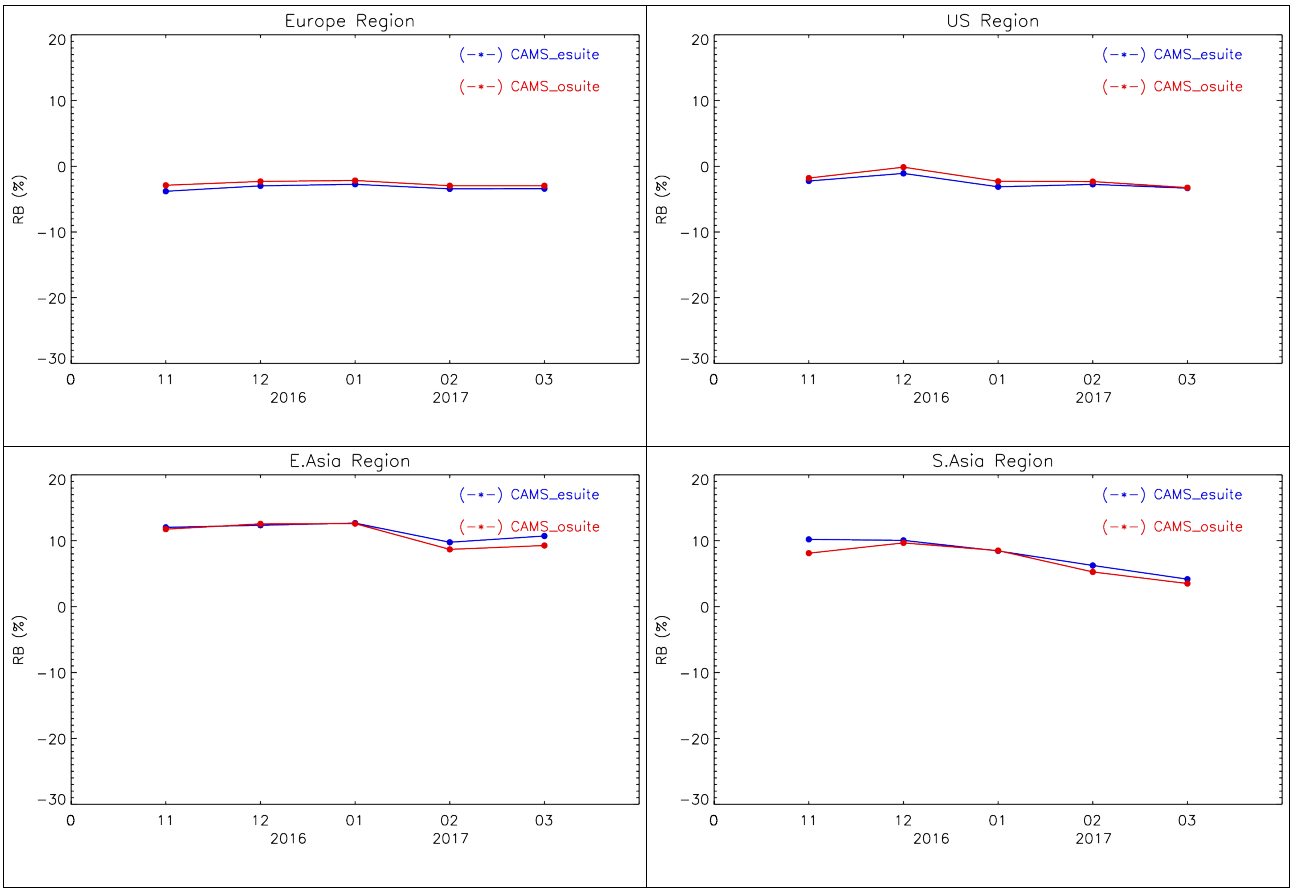

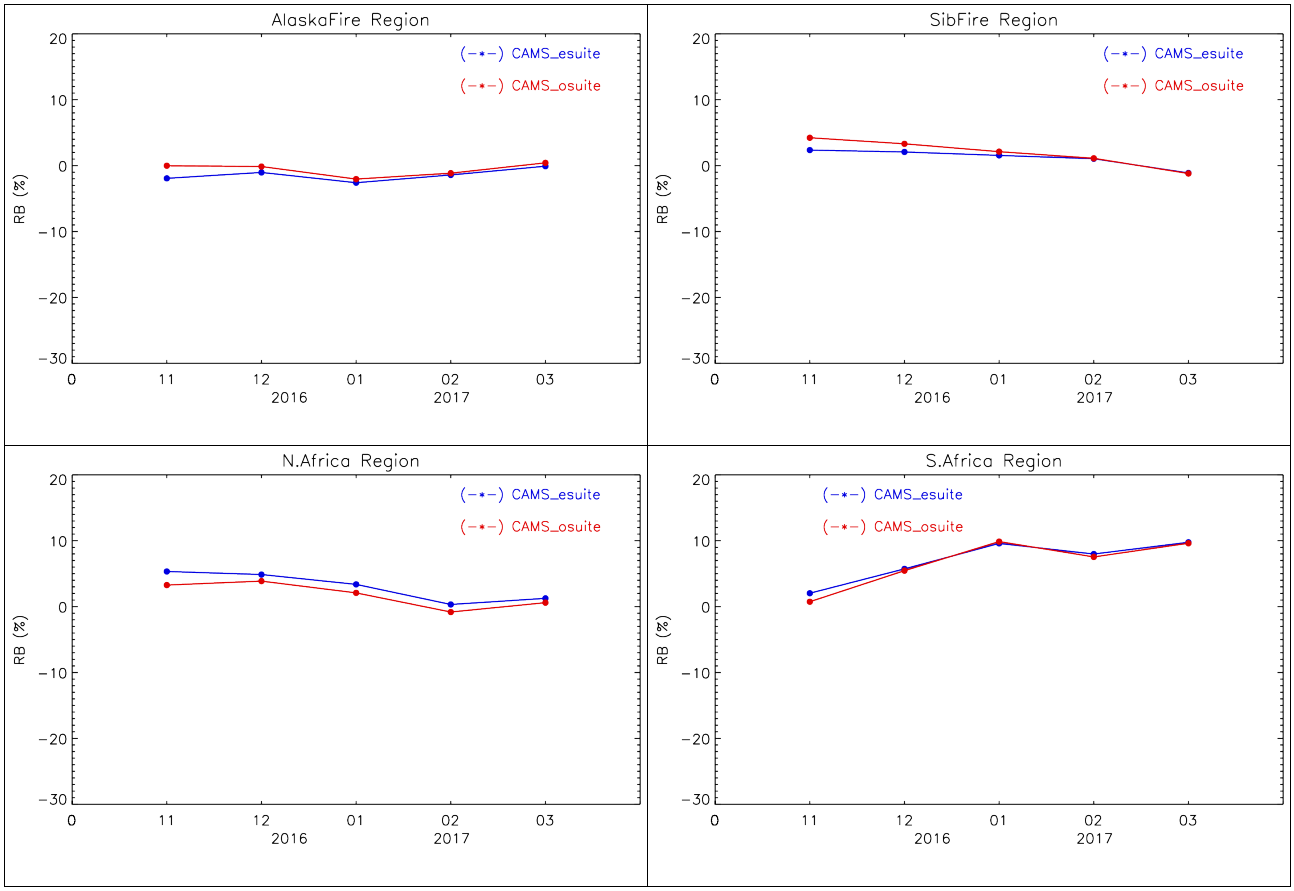

Fig.2.3.9: Bias in % of CAMS o-suite (red) and e-suite (blue) compared to MOPITTv6.

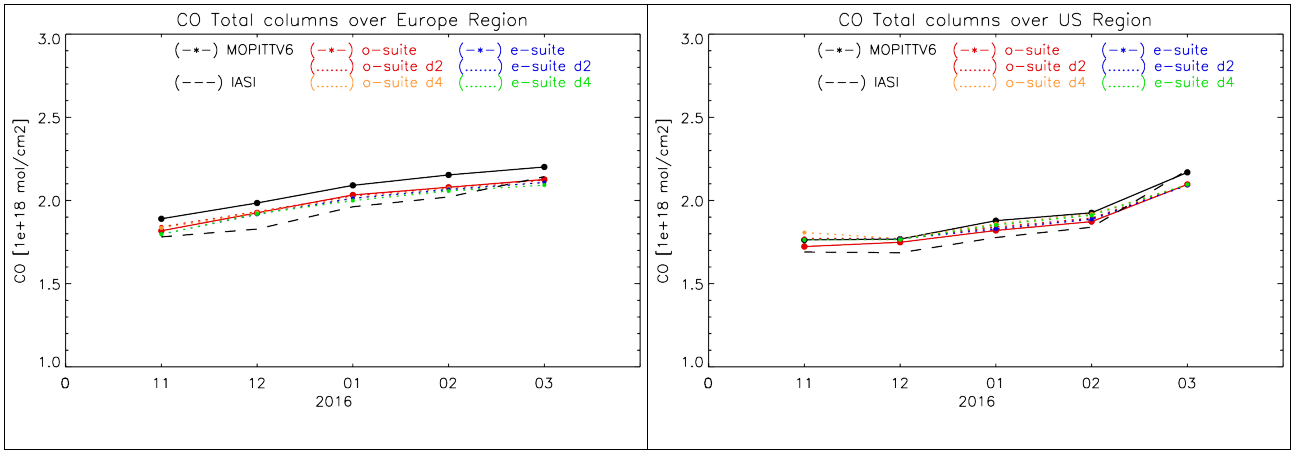

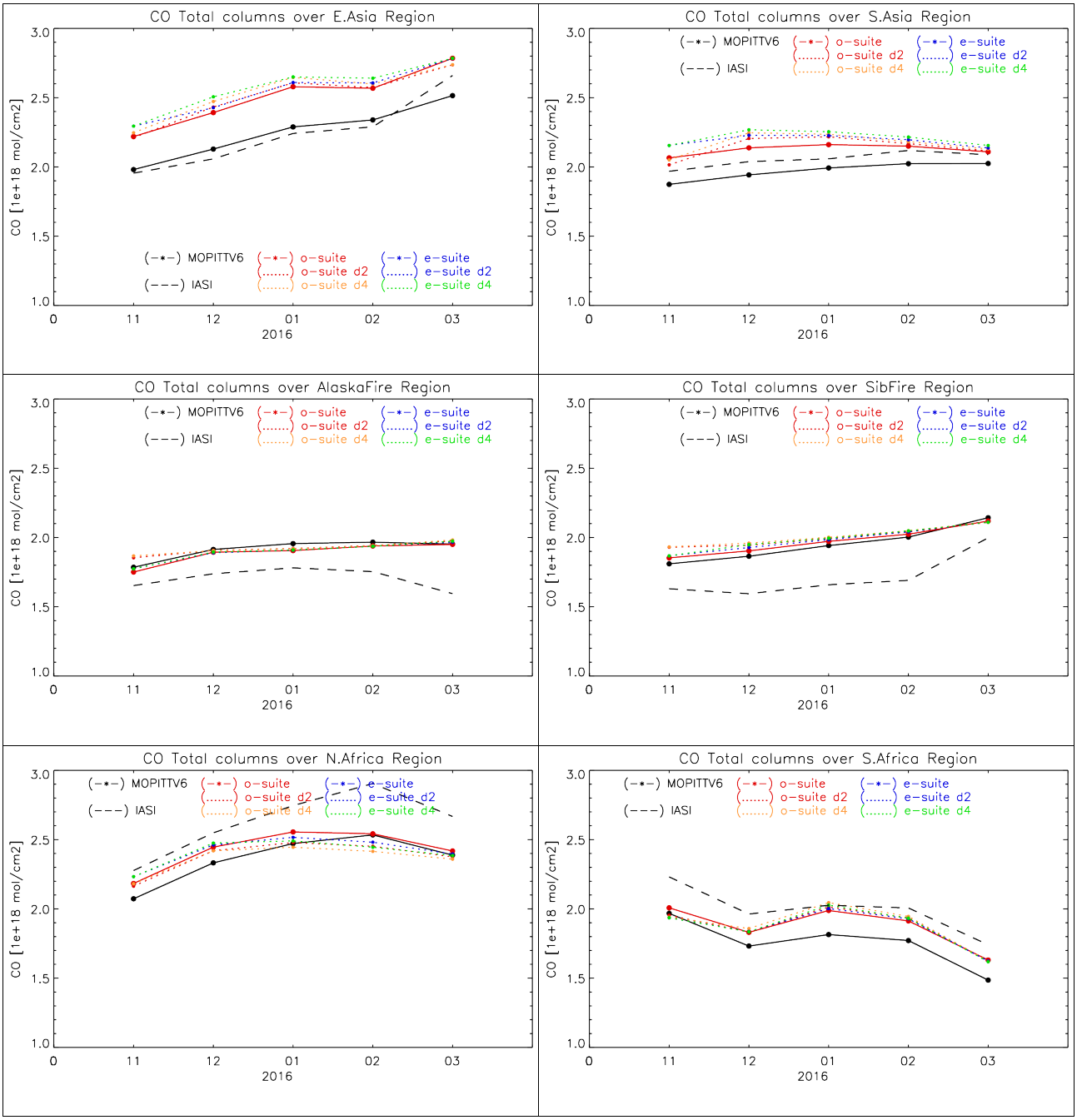

Fig. 2.3.10: Same as Fig.2.3.8, but also showing o-suite and e-suite forecast for day 2 and day 4.

2.4 Nitrogen dioxide

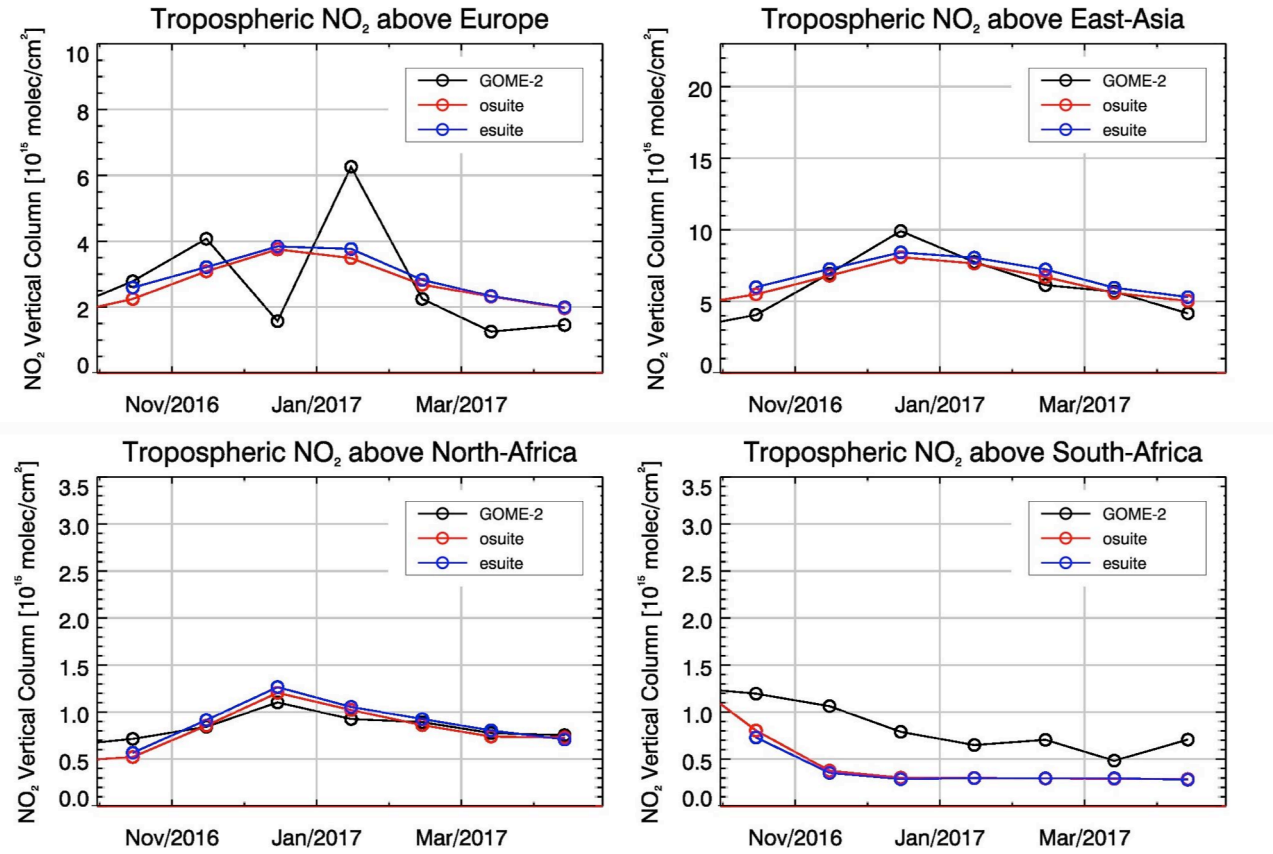

Figure 2.4.1: Time series of average tropospheric NO_2 columns [10^{15} molec cm^{-2}] from GOME-2 compared to model results for different regions.

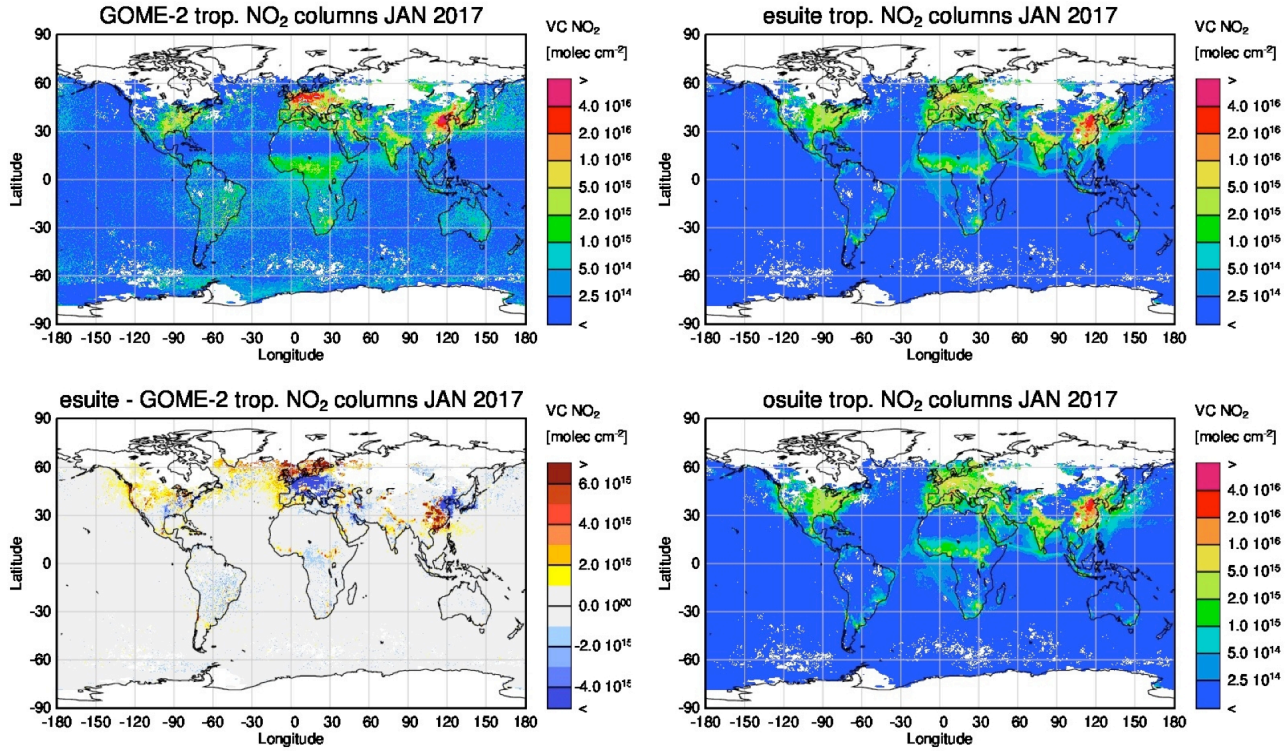

Figure 2.4.2: Monthly mean tropospheric NO_2 columns [molec cm^{-2}] from GOME-2 compared to model runs for January 2017. The top row shows GOME-2 and e-suite results, the lower one shows the difference between e-suite and GOME-2 as well as o-suite results. GOME-2 and model data were gridded to 0.4 degree resolution. Model data were treated with the same reference sector subtraction approach as the satellite data.

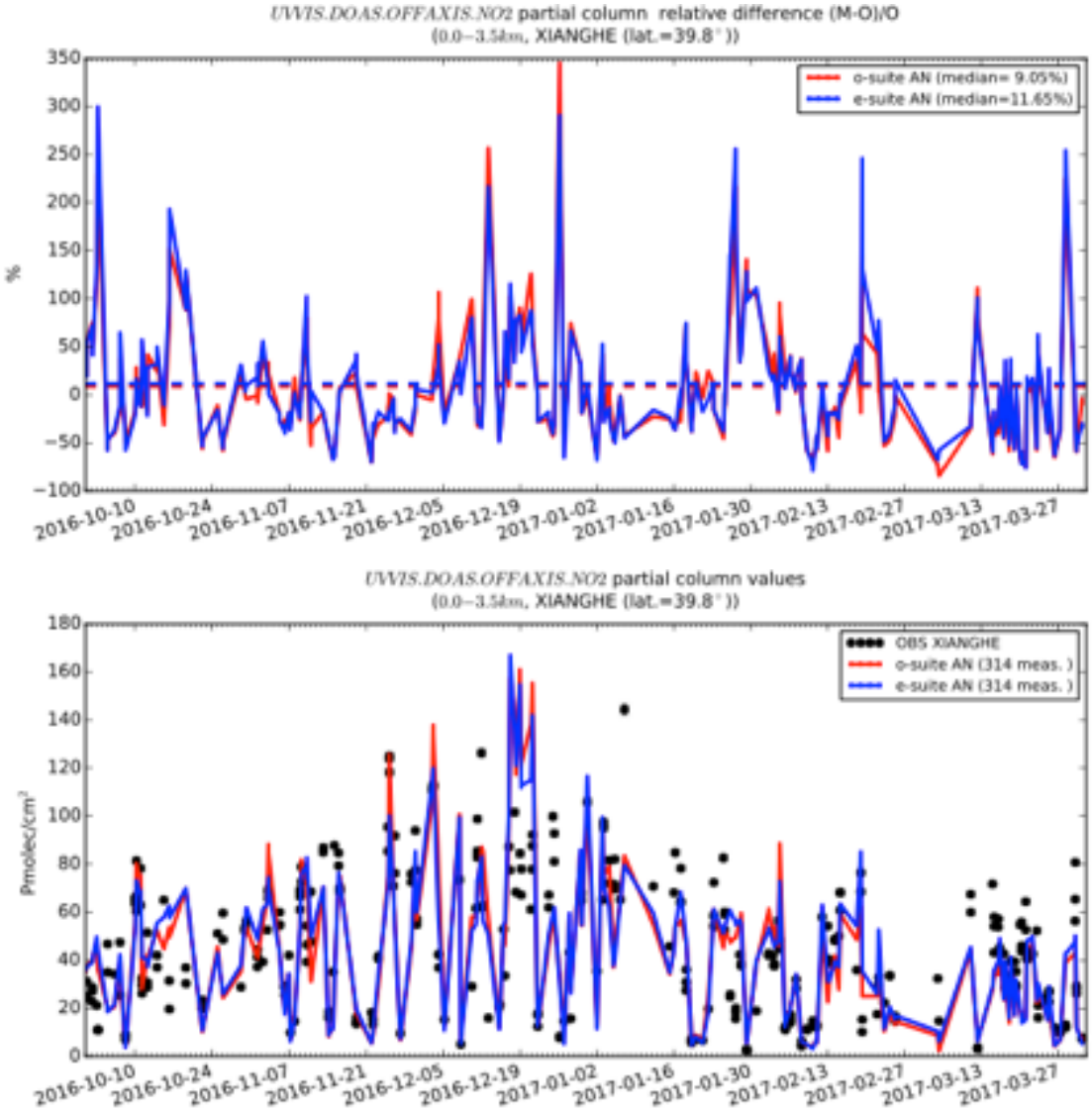

Fig. 2.4.3: Comparison of daily mean bias between the o- and e-suite NO2 partial column for the highly polluted Xianghe (Beijing) station. Little difference is observed, some high peak events show differences between o- and esuite

2.5 Formaldehyde (HCHO)

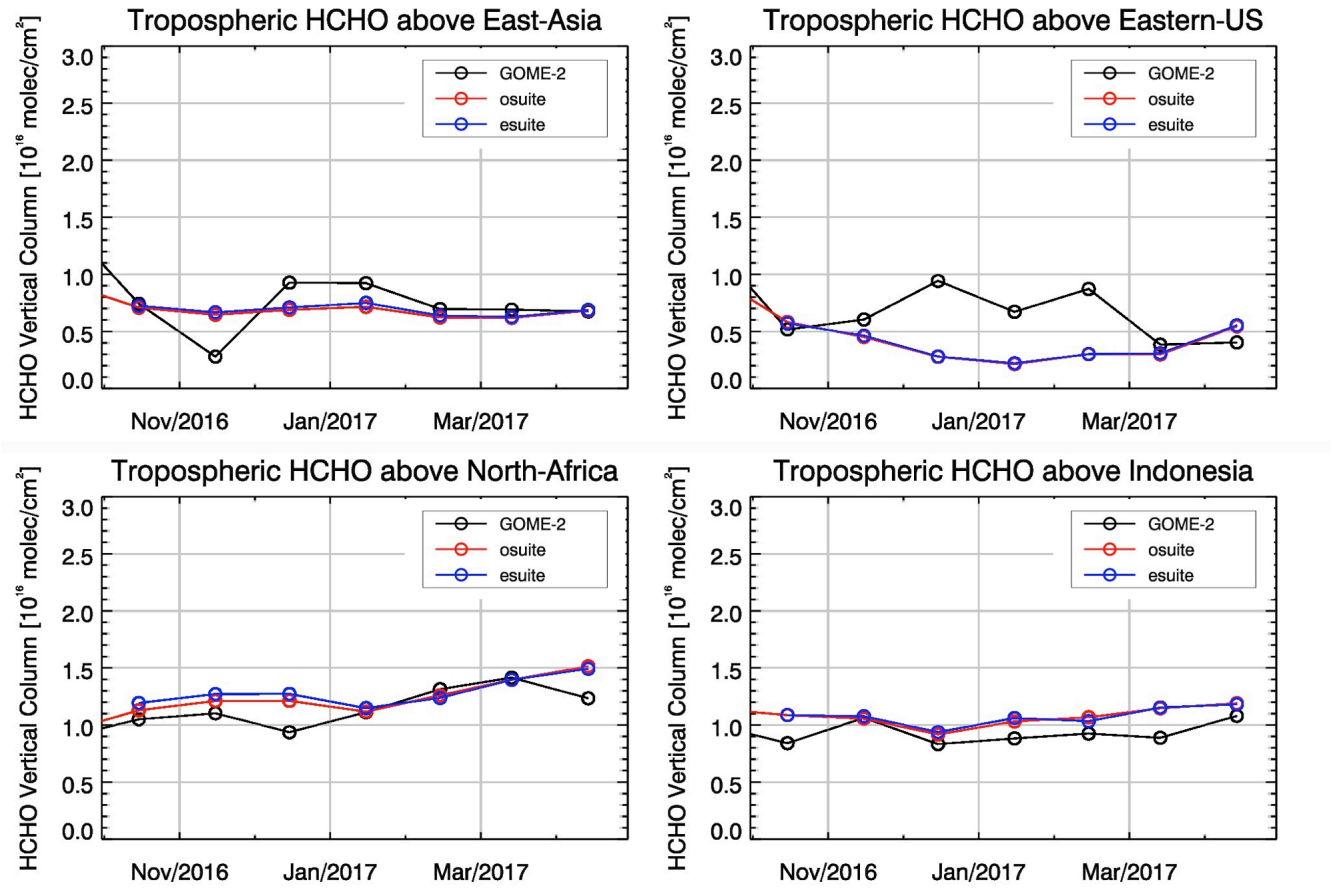

Figure 2.5.1: Time series of average tropospheric HCHO columns [10^{16} molec cm^{-2}] from GOME-2 compared to model results for different regions.

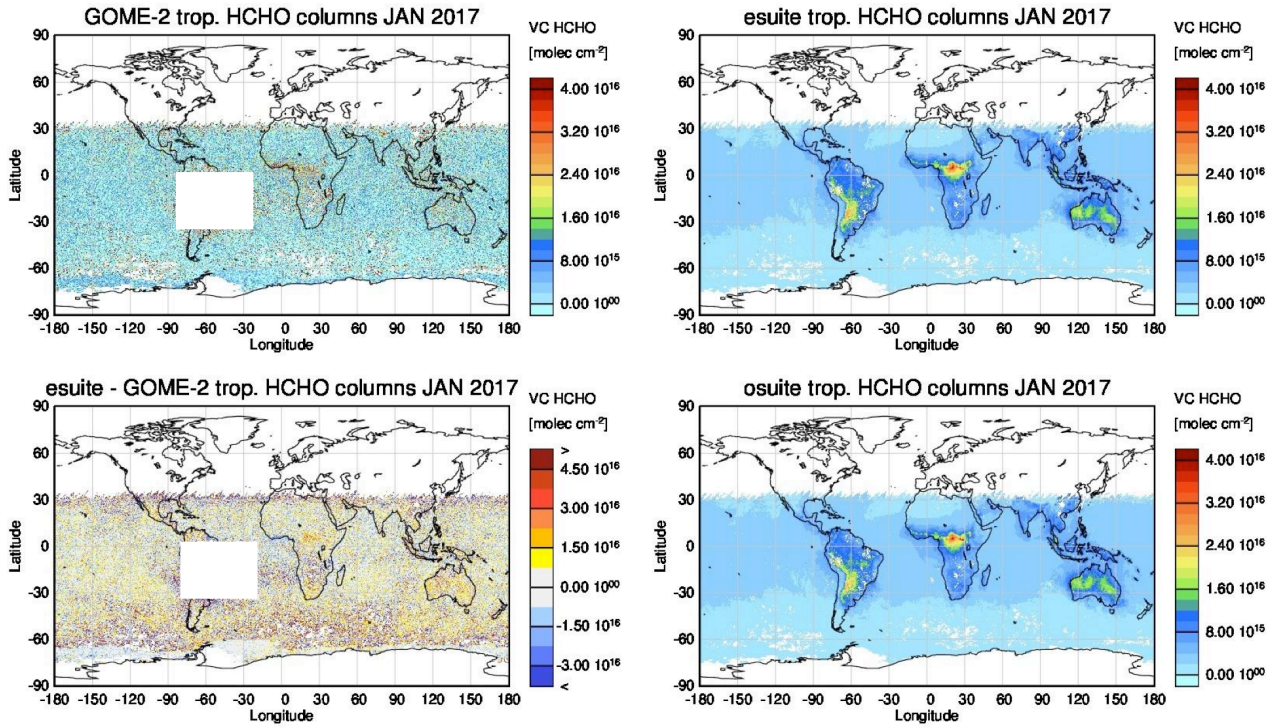

Figure 2.5.2: Monthly mean tropospheric HCHO columns [molec cm^{-2}] from GOME-2 compared to model runs for January 2017. The top row shows GOME-2 and esuite results, the lower one shows the difference between esuite and GOME-2 as well as osuite results. GOME-2 and model data were gridded to 0.4 degree resolution. Model data were treated with the same reference sector subtraction approach as the satellite data. Satellite retrievals in the region of the South Atlantic Anomaly are not valid and therefore masked out (white box in panels on the left).

2.6 Stratospheric ozone

2.6.1 Ozone sonde results

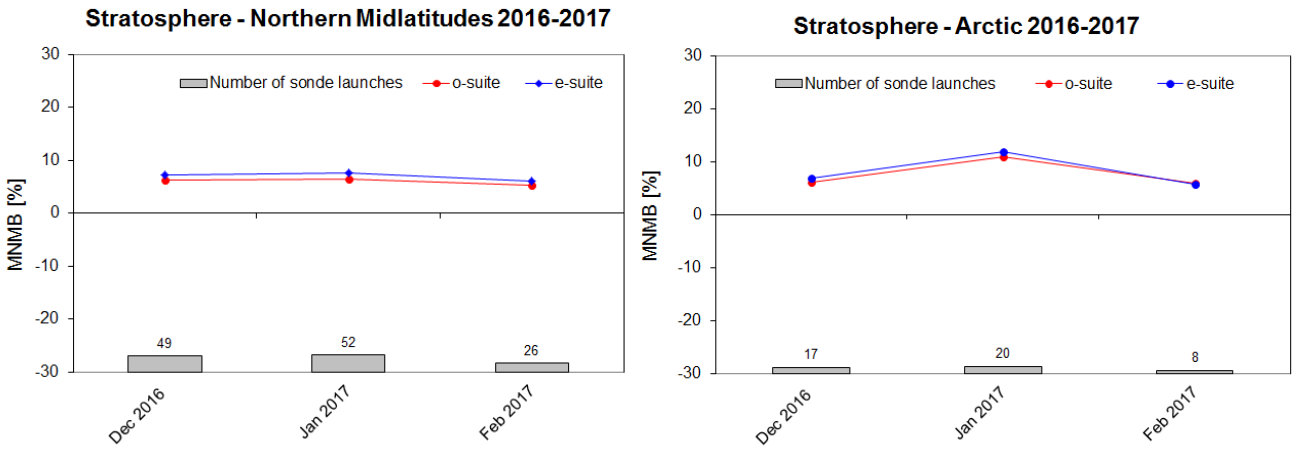

Fig. 2.6.1: MNMBs (%) of ozone in the stratosphere from the IFS model runs against aggregated sonde data over the Northern midlatiutdes (left) and the Arctic (right). The numbers indicate the amount of individual number of sondes.

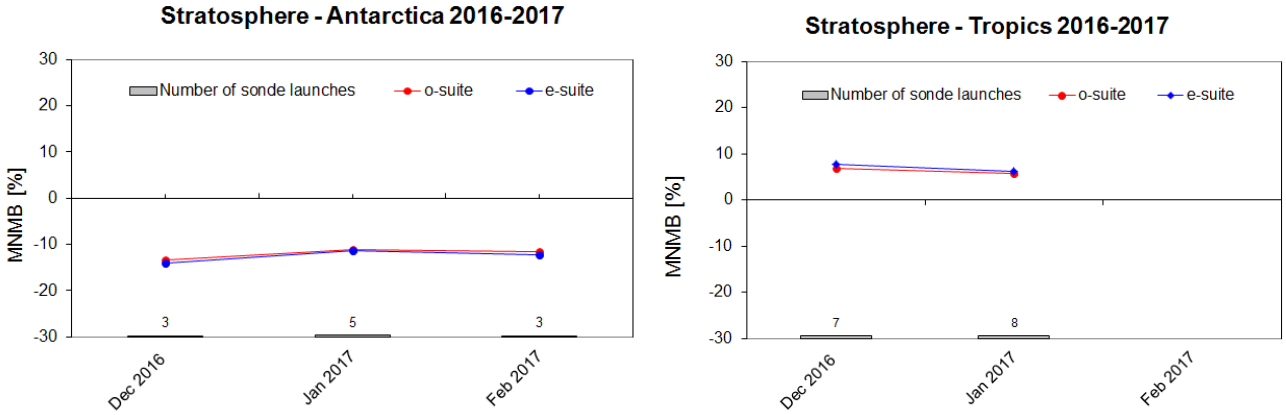

Fig. 2.6.2: MNMBs (%) of ozone in the stratosphere from the IFS model runs against aggregated sonde data over Antarctica (left) and the Tropics (right). The numbers indicate the amount of individual number of sondes.

2.6.2 Direct comparison with current o-suite

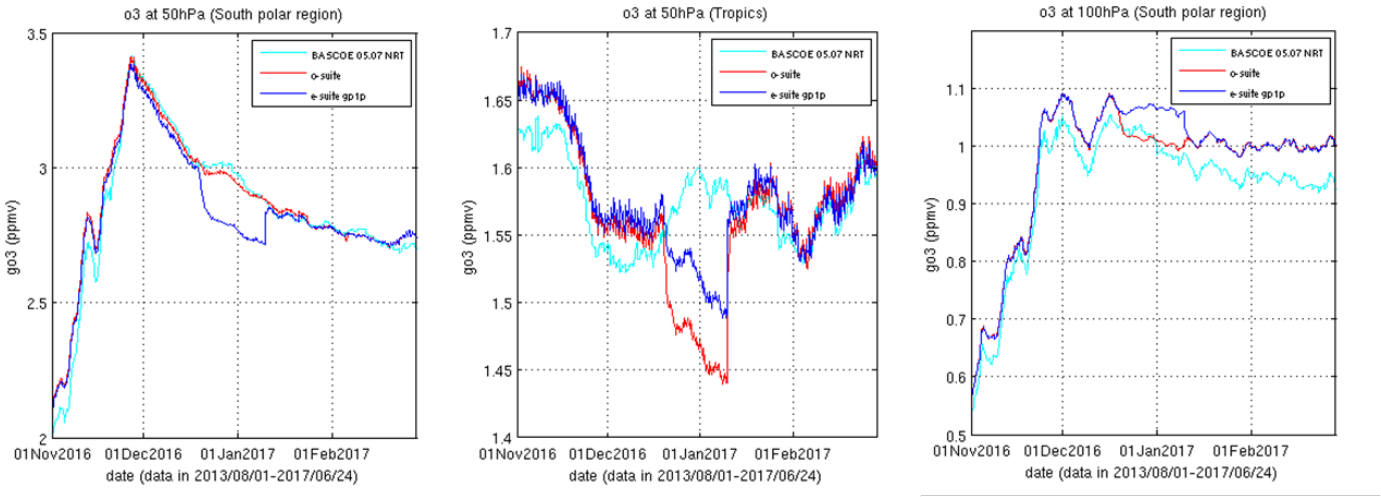

Figure 2.6.3: Comparison of zonal means of o-suite (red), e-suite gp1p (blue) and BASCOE NRT (cyan) for the period November 2016-February 2017, at 50hPa South polar region (left), at 50hPa tropics (center) and 100hPa South polar region (right).

2.6.3 Comparison with satellite observations

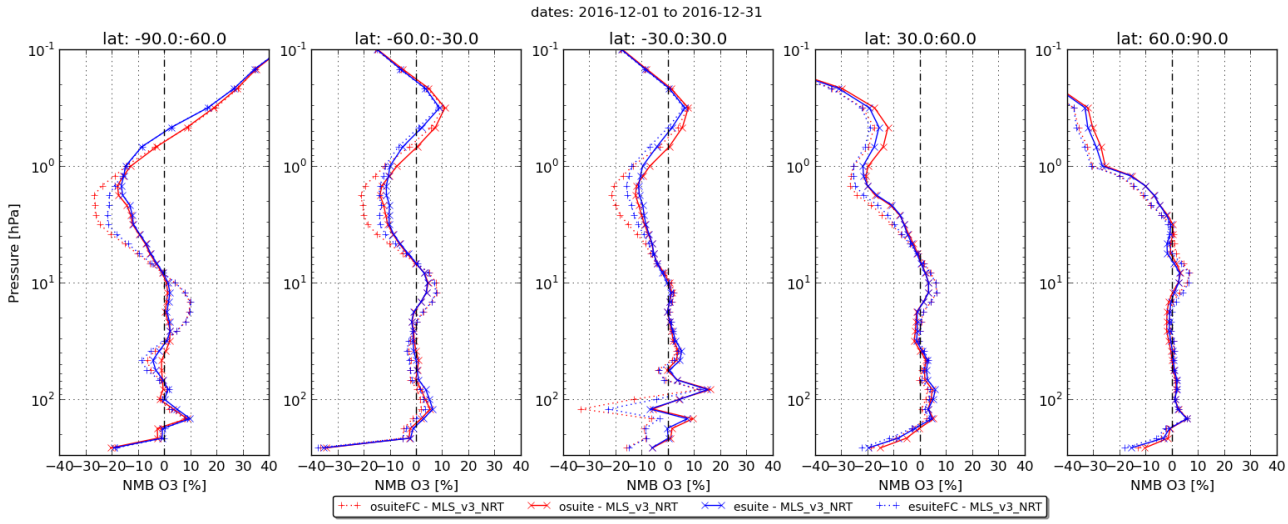

Figure 2.6.4: Mean normalized bias of o-suite (red) analyses (solid) and 4th day forecast (dotted) and e-suite (blue) analyses (solid) and 4th day forecast (dotted) w.r.t. AURA MLS NRT, for the month of December 2016. The analyses of the o-suite and the e-suite are very close in the range 1hPa to 100hPa; the 4th day forecast of the e-suite are closer to the observations in the upper stratosphere in the range of 1hPa to 6hPa.

2.6.4 Comparison with NDACC microwave observations

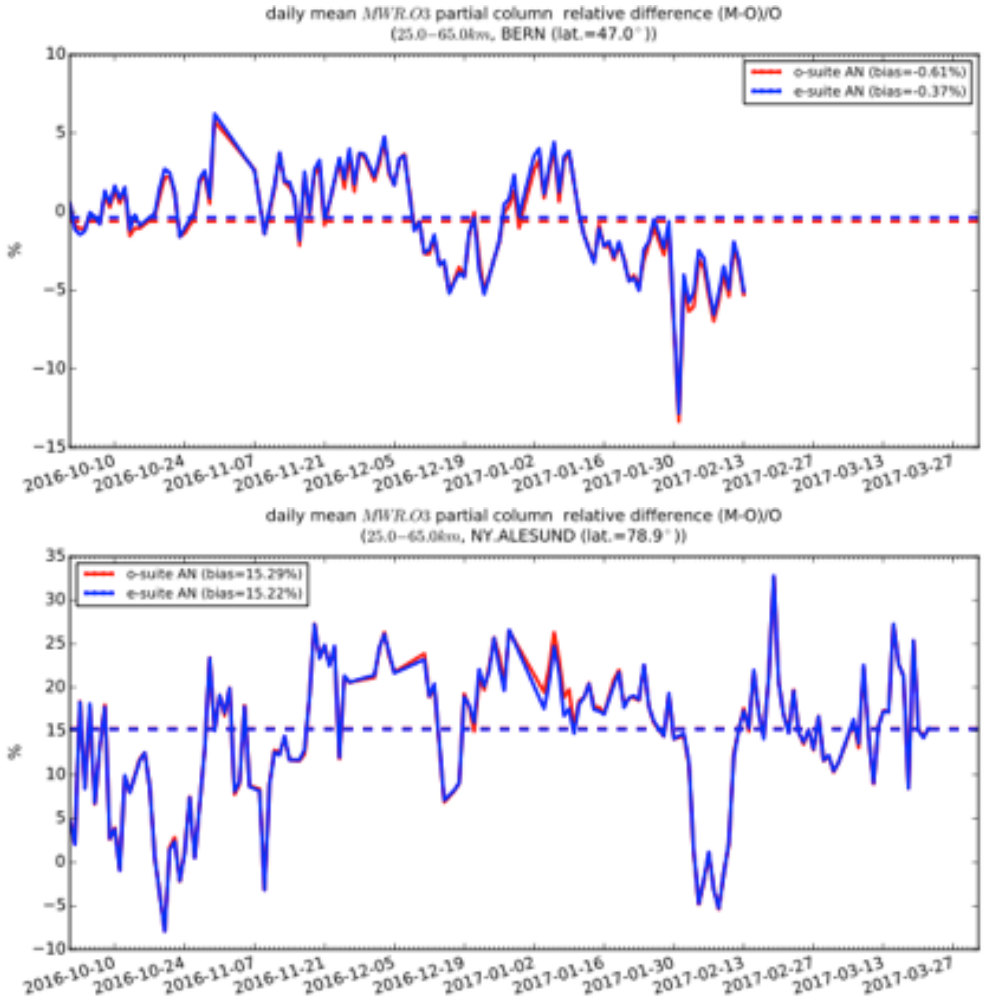

Fig. 2.6.5.: Comparison of daily mean bias between the o- and e-suite O3 partial column (25-65km) for the microwave observations of NDACC stations at Ny Alesund and Bern. The difference for this strato-/mesospheric column is very small.

2.7 Stratospheric NO2

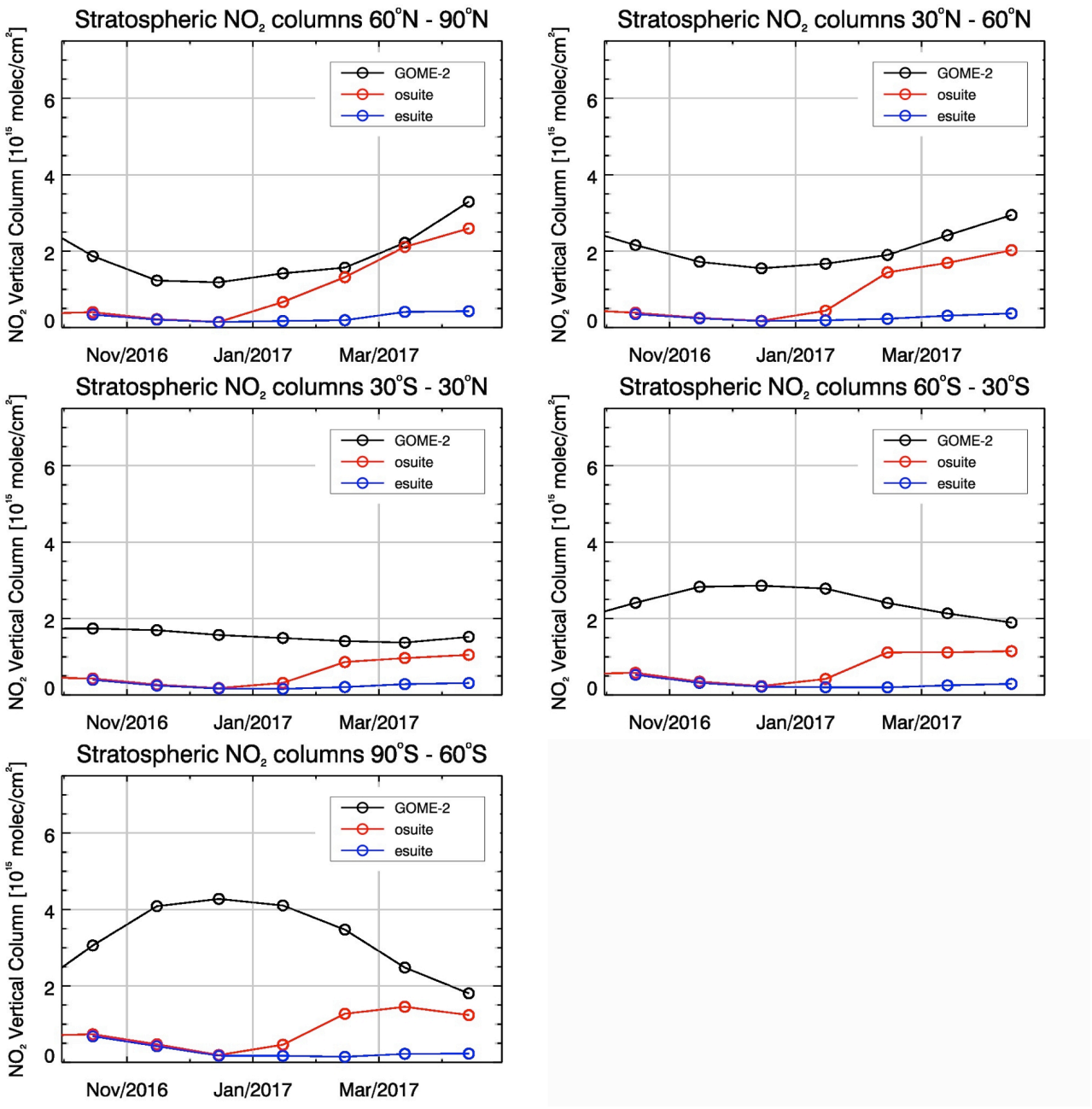

Figure 2.7.1: Time series of average stratospheric NO_2 columns [10^{15} molec cm-2] from GOME-2 compared to model results for different latitude bands.

2.8 Methane

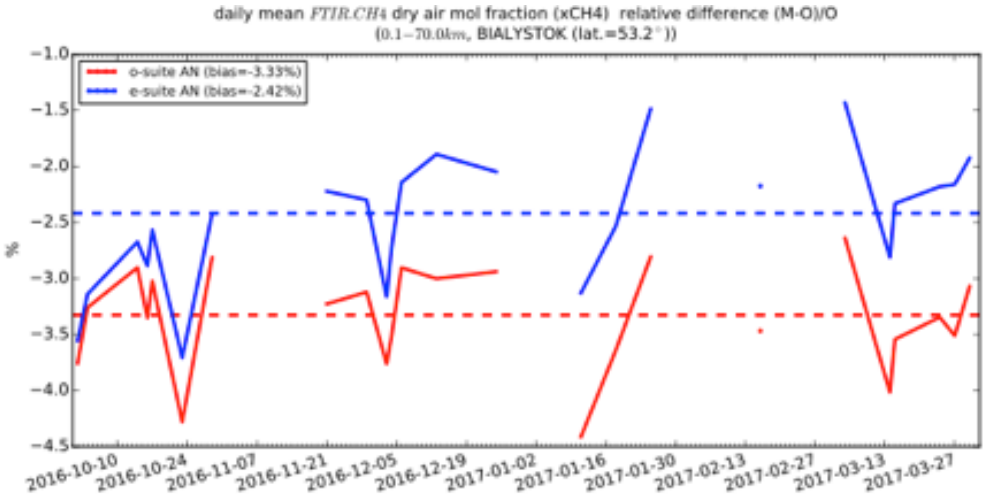
daily mean FTIR.CH4 dry air mol fraction (xCH4) relative difference (M-O)/O
(0.1−70.0km, BIALYSTOK (lat.=53.2°))
o-suite AN (bias=-3.33%)
e-suite AN (bias=-2.42%)
%
−1.0
−1.5
−2.0
−2.5
−3.0
−3.5
−4.0
−4.5
2016-10-10
2016-10-24
2016-11-07
2016-11-21
2016-12-05
2016-12-19
2017-01-02
2017-01-16
2017-01-30
2017-02-13
2017-02-27
2017-03-13
2017-03-27

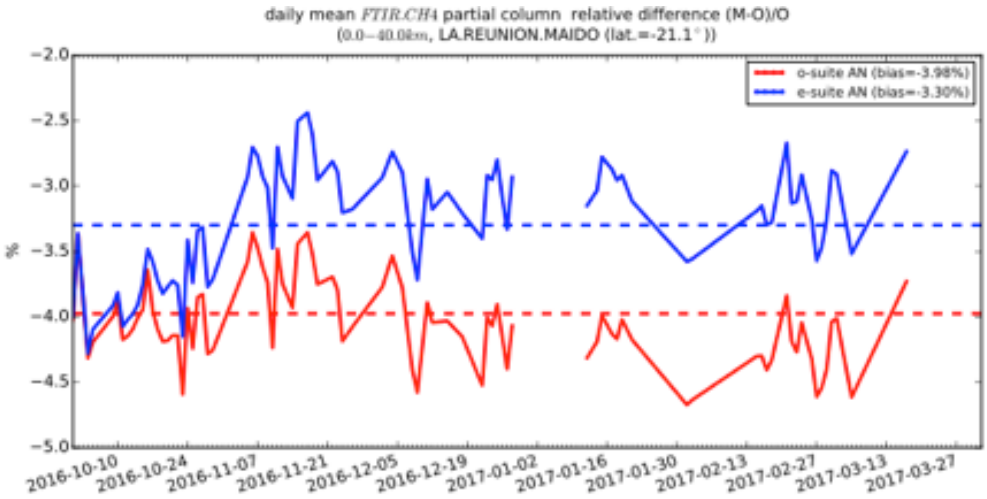
daily mean FTIR.CH4 partial column relative difference (M-O)/O
(0.0−40.0km, LA.REUNION.MAIDO (lat.=-21.1°))
o-suite AN (bias=-3.98%)
e-suite AN (bias=-3.30%)
%
−2.0
−2.5
−3.0
−3.5
−4.0
−4.5
−5.0
2016-10-10
2016-10-24
2016-11-07
2016-11-21
2016-12-05
2016-12-19
2017-01-02
2017-01-16
2017-01-30
2017-02-13
2017-02-27
2017-03-13
2017-03-27

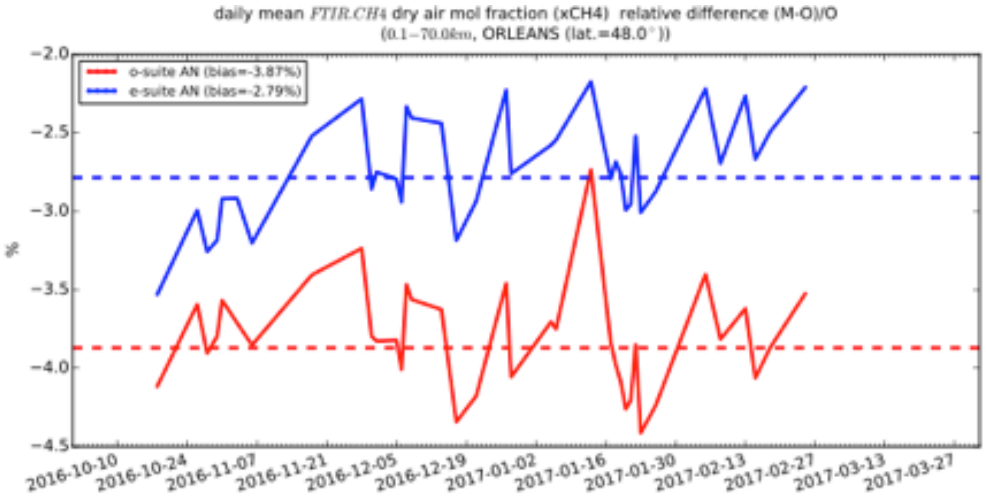
daily mean FTIR.CH4 dry air mol fraction (xCH4) relative difference (M-O)/O
(0.1−70.0km, ORLEANS (lat.=48.0°))
o-suite AN (bias=-3.87%)
e-suite AN (bias=-2.79%)
%
−2.0
−2.5
−3.0
−3.5
−4.0
−4.5
2016-10-10
2016-10-24
2016-11-07
2016-11-21
2016-12-05
2016-12-19
2017-01-02
2017-01-16
2017-01-30
2017-02-13
2017-02-27
2017-03-13
2017-03-27

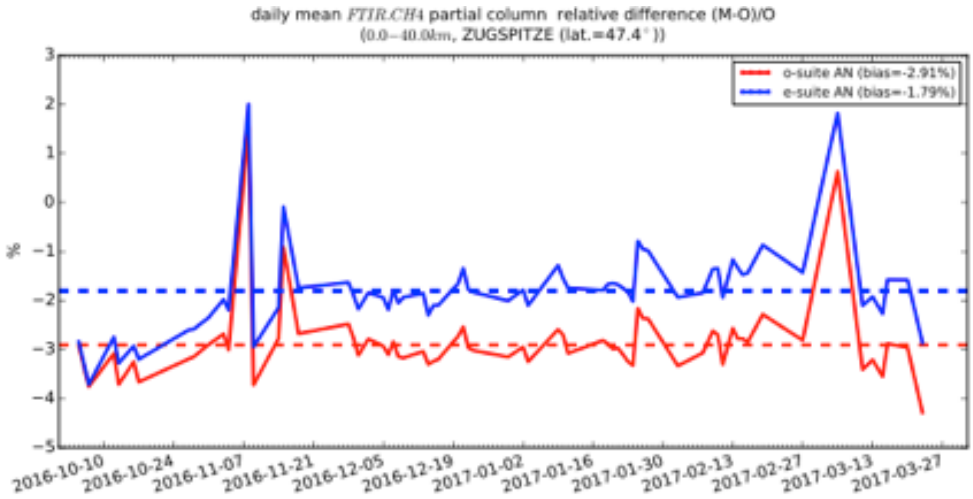

Fig. 2.8.1: Comparison of daily mean bias between the o- and e-suite CH4 partial column for the TCCON stations Bialystok and Orleans (left) and the NDACC stations at Reunion and Toronto (right). E-suite reduces the bias at all sites from 3-4% to values below 3%.

3. References

Benedetti, A., J.-J. Morcrette, O. Boucher, A. Dethof, R. J. Engelen, M. Fisher, H. Flentjes, N. Huneeus, L. Jones, J. W. Kaiser, S. Kinne, A. Mangold, M. Razinger, A. J. Simmons, M. Suttie, and the GEMS-AER team: Aerosol analysis and forecast in the ECMWF Integrated Forecast System. Part II : Data assimilation, J. Geophys. Res., 114, D13205, doi:10.1029/2008JD011115, 2009.

Cariolle, D. and Teyssèdre, H.: A revised linear ozone photochemistry parameterization for use in transport and general circulation models: multi-annual simulations, Atmos. Chem. Phys., 7, 2183-2196, doi:10.5194/acp-7-2183-2007, 2007.

Dee, D. P. and S. Uppala, Variational bias correction of satellite radiance data in the ERA-Interim reanalysis. Quart. J. Roy. Meteor. Soc.,135, 1830-1841, 2009.

Eskes, H., Huijnen, V., Arola, A., Benedictow, A., Blechschmidt, A.-M., Botek, E., Boucher, O., Bouarar, I., Chabrillat, S., Cuevas, E., Engelen, R., Flentje, H., Gaudel, A., Griesfeller, J., Jones, L., Kapsomenakis, J., Katragkou, E., Kinne, S., Langerock, B., Razinger, M., Richter, A., Schultz, M., Schulz, M., Sudarchikova, N., Thouret, V., Vrekoussis, M., Wagner, A., and Zerefos, C.: Validation of reactive gases and aerosols in the MACC global analysis and forecast system, Geosci. Model Dev., 8, 3523-3543, doi:10.5194/gmd-8-3523-2015, 2015.

Eskes, H.J., V. Huijnen, S, Basart, A. Benedictow, A.-M. Blechschmidt, S. Chabrillat, H. Clark, Y. Christophe, E. Cuevas, H. Flentje, K. M. Hansen, J. Kapsomenakis, B. Langerock, M. Ramonet, A. Richter, M. Schulz, A. Wagner, T. Warneke, C. Zerefos: Observations characterisation and validation methods document. Copernicus Atmosphere Monitoring Service (CAMS) report, CAMS84_2015SC1_D84.8.1_2016Q2_201603, March 2016. Available from: http://atmosphere.copernicus.eu/user-support/validation/verification-global-services

Eskes, H.J., A. Wagner, M. Schulz, Y. Christophe, M. Ramonet, S. Basart, A. Benedictow, A.-M. Blechschmidt, S. Chabrillat, H. Clark, E. Cuevas, H. Flentje, K.M. Hansen, U. Im, J. Kapsomenakis, B. Langerock, K. PetersEN, A. Richter, N. Sudarchikova, V. Thouret, T. Warneke, C. Zerefos, Validation report of the CAMS near-real-time global atmospheric composition service: December 2016 - February 2017, Copernicus Atmosphere Monitoring Service (CAMS) report, CAMS84_2015SC2_D84.1.1.7_2017DJF_v1.pdf, May 2017.

Flemming, J., Huijnen, V., Arteta, J., Bechtold, P., Beljaars, A., Blechschmidt, A.-M., Diamantakis, M., Engelen, R. J., Gaudel, A., Inness, A., Jones, L., Josse, B., Katragkou, E., Marecal, V., Peuch, V.-H., Richter, A., Schultz, M. G., Stein, O., and Tsikerdekis, A.: Tropospheric chemistry in the Integrated Forecasting System of ECMWF, Geosci. Model Dev., 8, 975-1003, doi:10.5194/gmd-8-975-2015, 2015.

Granier, C. et al.: Evolution of anthropogenic and biomass burning emissions of air pollutants at global and regional scales during the 1980–2010 period. Climatic Change (109), 2011.

Huijnen, V., et al.: The global chemistry transport model TM5: description and evaluation of the tropospheric chemistry version 3.0, Geosci. Model Dev., 3, 445-473, doi:10.5194/gmd-3-445-2010, 2010.

Inness, A., Blechschmidt, A.-M., Bouarar, I., Chabrillat, S., Crepulja, M., Engelen, R. J., Eskes, H., Flemming, J., Gaudel, A., Hendrick, F., Huijnen, V., Jones, L., Kapsomenakis, J., Katragkou, E., Keppens, A., Langerock, B., de Mazière, M., Melas, D., Parrington, M., Peuch, V. H., Razinger, M., Richter, A., Schultz, M. G., Suttie, M., Thouret, V., Vrekoussis, M., Wagner, A., and Zerefos, C.: Data assimilation of satellite-retrieved ozone, carbon monoxide and nitrogen dioxide with ECMWF's Composition-IFS, Atmos. Chem. Phys., 15, 5275-5303, doi:10.5194/acp-15-5275-2015, 2015.

Kaiser, J. W., Heil, A., Andreae, M. O., Benedetti, A., Chubarova, N., Jones, L., Morcrette, J.-J., Razinger, M., Schultz, M. G., Suttie, M., and van der Werf, G. R.: Biomass burning emissions estimated with a global fire assimilation system based on observed fire radiative power, Biogeosciences, 9, 527-554, doi:10.5194/bg-9-527-2012, 2012.

Morcrette, J.-J., O. Boucher, L. Jones, D. Salmond, P. Bechtold, A. Beljaars, A. Benedetti, A. Bonet, J. W. Kaiser, M. Razinger, M. Schulz, S. Serrar, A. J. Simmons, M. Sofiev, M. Suttie, A. M. Tompkins, and A. Untch: Aerosol analysis and forecast in the ECMWF Integrated Forecast System. Part I: Forward modelling, J. Geophys. Res., 114, D06206, doi:10.1029/2008JD011235, 2009.

Annex 1: Acknowledgements for measurements used

We wish to acknowledge the provision of NRT GAW observational data by: Institute of Atmospheric Sciences and Climate (ISAC) of the Italian National Research Council (CNR), South African Weather Service, National Centre for Atmospheric Science (NCAS, Cape Verde), National Air Pollution Monitoring Network (NABEL) (Federal Office for the Environment FOEN and Swiss Federal Laboratories for Materials Testing and Research EMPA), Atmospheric Environment Division Global Environment and Marine Department Japan Meteorological Agency, Chinese Academy of Meteorological Sciences (CAMS), Alfred Wegener Institut, Umweltbundesamt (Austria), National Meteorological Service (Argentina), Umweltbundesamt (UBA, Germany)

We are grateful to the numerous operators of the Aeronet network and to the central data processing facility at NASA Goddard Space Flight Center for providing the NRT sun photometer data, especially Ilya Slutker and Brent Holben for sending the data.

The authors thank to all researchers, data providers and collaborators of the World Meteorological Organization's Sand and Dust Storm Warning Advisory and Assessment System (WMO SDS-WAS) for Northern Africa, Middle East and Europe (NAMEE) Regional Node. Also special thank to Canary Government as well as AERONET, MODIS, U.K. Met Office MSG, MSG Eumetsat and EOSDIS World Viewer principal investigators and scientists for establishing and maintaining data used in the activities of the WMO SDS-WAS NAMEE Regional Center (http://sds-was.aemet.es/).

We wish to acknowledge the provision of ozone sonde data by the World Ozone and Ultraviolet Radiation Data Centre established at EC in Toronto (http://woudc.org), by the Data Host Facility of the Network for the Detection of Atmospheric Composition Change established at NOAA (http://ndacc.org), by the Norwegian Institute for Air Research and by the National Aeronautics and Space Administration (NASA).

We wish to thank the NDACC investigators for the provision of observations at Ny Alesund, Bern, Jungfraujoch, Izaña, Xianghe, Harestua, Reunion Maido, Uccle, Hohenpeissen, Mauna Loa, Lauder and Haute Provence. Special thanks to the data providers at Ny-Alesund, Bern and Uccle for their support of the Arctic ozone depletion case study.

The authors acknowledge the NOAA Earth System Research Laboratory (ESRL) Global Monitoring Division (GMD) for the provision of ground based ozone concentrations.

The MOPITT CO data were obtained from the NASA Langley Research Center ASDC. We acknowledge the LATMOS IASI group for providing IASI CO data.

SCIAMACHY lv1 radiances were provided to IUP-UB by ESA through DLR/DFD.

GOME-2 lv1 radiances were provided to IUP-UB by EUMETSAT.

The authors acknowledge Environment and Climate Change Canada for the provision of Alert ozone data and Sara Crepinsek – NOAA for the provision of Tiksi ozone data. Surface ozone data from the Villum Research Station, Station Nord (VRS) was financially supported by "The Danish

Environmental Protection Agency" with means from the MIKA/DANCEA funds for Environmental Support to the Arctic Region. The Villum Foundation is acknowledged for the large grant making it possible to build VRS in North Greenland.

We acknowledge the National Aeronautics and Space Administration (NASA), USA for providing the http://osirus.usask.ca/OMPS limb sounder data (http://npp.gsfc.nasa.gov/omps.html) and the Aura-MLS offline data (http://mls.jpl.nasa.gov/index-eos-mls.php).

We thank the University of Saskatchewan, Canada for providing the OSIRIS (http://osirus.usas.ca/) observations data and the Canadian Space Agency and ACE science team for providing level 2 data retrieved from ACE-FTS on the Canadian satellite SCISAT-1.

The TCCON site at Orleans is operated by the University of Bremen and the RAMCES team at LSCE (Gif-sur-Yvette, France). The TCCON site at Bialystok is operated by the University of Bremen. Funding for the two sites was provided by the EU-project ICOS-INWIRE and the University of Bremen. The TCCON site at Réunion is operated by BIRA-IASB, in cooperation with UReunion and is funded by BELSPO in the framework of the Belgian ICOS program.

The European Environment Information and Observation Network (Eionet) Air Quality portal provides details relevant for the reporting of air quality information from EU Member States and other EEA member and co-operating countries. This information is submitted according to Directives 2004/107/EC and 2008/50/EC of the European Parliament and of the Council.

Copernicus Atmosphere Monitoring Service

ECMWF - Shinfield Park, Reading RG2 9AX, UK

Contact: info@copernicus-atmosphere.eu